NASA TECHNICAL NOTE

NASA TN D-4662

THRUST-VECTOR CONTROL REQUIREMENTS FOR LARGE LAUNCH VEHICLES WITH SOLID-PROPELLANT FIRST STAGES

by Fred Teren, Kenneth I. Davidson, Janos Borsody, and Carl J. Daniele

Lewis Research Center
Cleveland, Ohio

NATIONAL AERONAUTICS AND SPACE ADMINISTRATION • WASHINGTON, D. C. • JULY 1968

THRUST-VECTOR CONTROL REQUIREMENTS FOR LARGE LAUNCH VEHICLES WITH SOLID-PROPELLANT FIRST STAGES

By Fred Teren, Kenneth I. Davidson, Janos Borsody, and Carl J. Daniele

Lewis Research Center
Cleveland, Ohio

NATIONAL AERONAUTICS AND SPACE ADMINISTRATION

For sale by the Clearinghouse for Federal Scientific and Technical Information
Springfield, Virginia 22151 – CFSTI price $3.00

ABSTRACT

Thrust vector deflection (TVD) requirements are calculated for control of two solid-based launch vehicles - the 260-inch solid-SIVB (with a family of payload shapes and densities) and a large two-stage clustered solid vehicle (SSOPM) designed to deliver 450 000 kg of payload to orbit. TVD requirements for 99 percent wind loads were found to be 2.4^{o} and 1.17^{o} for 260-inch solid-SIVB and SSOPM, respectively. Requirements for other effects added about 0.35^{o} for both vehicles. About 1^{o} of TVD is required for control during tailoff for SSOPM. The TVD requirements for winds are reduced by using stationary base fins or movable canards.

STAR Category 31

THRUST-VECTOR CONTROL REQUIREMENTS FOR LARGE LAUNCH VEHICLES WITH SOLID-PROPELLANT FIRST STAGES

by Fred Teren, Kenneth I. Davidson, Janos Borsody, and Carl J. Daniele

Lewis Research Center

SUMMARY

Thrust vector deflection (TVD) requirements are calculated for control of solid-based launch vehicles. Two launch vehicles were considered. The first is the 260-inch solid-SIVB launch vehicle with both the Apollo and extended Voyager payloads. In addition, a family of shroud shapes and densities is studied to determine the effects of these parameters on TVD requirements. The second vehicle considered (SSOPM) consists of a cluster of seven 260-inch solid motors in the first stage and a solid propellant second stage. This vehicle is designed to deliver 450 000 kilograms of payload to a 185 kilometers circular orbit.

In the first part of the study, pitch and yaw TVD requirements are calculated for 99 percent wind loads. It was found that about 2.30° and 1.35° are required for the 260-inch solid vehicle with the Voyager and Apollo payloads, respectively. The SSOPM requirement is 1.17°. The analysis of several payload densities and shapes on the 260-inch solid-SIVB launch vehicle resulted in TVD wind requirements of less than 2.4° for payload densities greater than 70.2 kilograms per cubic meter. The TVD required for effects other than winds is also briefly discussed and is found to add about 0.35° to the wind requirement. The TVD required for control during tailoff was found to be about 1° for the SSOPM vehicle.

The second part of the study is concerned with reducing the TVD requirement for winds by use of base fins or movable canards. It was found that the 260-inch solid-Voyager TVD requirement could be reduced to 0.5° by using base fins or canards with total area of 1.4 or 0.7 times the vehicle base area, respectively. The required surface areas for the other vehicles are smaller. The advantages and disadvantages of using fins and canards are discussed. In particular, the reduction in the vehicle bending moments obtainable with canards is presented.

The results obtained in this report cannot be generalized to other vehicles. However, some trends are established; and the significant study variables and procedures are determined.

INTRODUCTION

The problem of obtaining thrust vector deflection (TVD) is not difficult for liquid propellant rockets since the combustion chamber and exhaust nozzle can be gimbaled as a unit. For solid propellant rockets however, the solid motor and propellant casing form an integral unit so that engine gimbaling is impractical. The nozzle can be gimbaled, but such a mechanization can be both complicated and costly. Secondary liquid injection has been studied as a possible method for obtaining TVD (ref. 1). With this method, the amount of TVD obtainable is adequate; but a significant payload penalty may be suffered due to the weight of liquid injectants which must be carried in flight. Because of these factors, it is important to establish and minimize the TVD requirements for solid propellant launch vehicles.

A unique approach has been studied in reference 2; that of reducing the TVD requirements by making use of the vehicle stability limit. In this reference, it is shown that TVD requirements can be reduced by as much as 50 percent by using an idealized load relief autopilot design. However no attempt is made to design a realistic autopilot to determine if comparable results can be obtained. A drawback to this method is the resulting large dispersions at booster cutoff. These dispersions can lead to upper stage guidance problems and/or payload losses.

The purpose of the present report is to establish and minimize TVD requirements for several typical solid propellant vehicles. The effectiveness of passive and active aerodynamic control surfaces in reducing TVD requirements is studied. The passive control surfaces studied consist of a set of eight fins mounted symmetrically about the base of the vehicle. The shape of the fins is the same as used on Saturn IB, as described in a work entitled "Aerodynamics of the Saturn IB Redesigned Fin" by Bob G. Dunn of the NASA Marshall Space Flight Center. The size of the fins is varied parametrically for each configuration studied herein. The active control surfaces studied consist of four canards symmetrically mounted near the nose of the vehicle. The canards are similar to those studied for the Atlas-Centaur configuration (ref. 3).

In order to simplify the calculation of TVD requirements, the trajectory is assumed to be unchanged from the nominal (no drift) due to the presence of a wind disturbance. The angle of attack profile due to the disturbance can then be calculated by superimposing the wind profile on the trajectory. Since the trajectory is flown trimmed to the nominal pitch profile, TVD requirements are then calculated as the amount necessary to cancel the aerodynamic moment. The TVD requirements resulting from the no drift assumption are verified by detailed six degree of freedom simulations presented herein, as well as by the results presented in reference 2.

Results are presented for two launch vehicles and a family of payload shapes. The first vehicle is the uprated Saturn IB (ref. 1) consisting of a single 260-inch solid motor for the first stage and the SIVB second stage. Two definite payloads are considered-the

Apollo (command module, service module, and LEM adapter) and the extended Voyager payloads. In addition, a family of payload shapes and the densities is considered to determine the effect of these parameters on TVD requirements. The second vehicle studied, referred to as SSOPM, consists of a booster stage with seven 260-inch (6.61 m) solid motors, and a solid propellant second stage. The vehicle also includes an orbital propulsion module plus the payload, assumed to have a density of 64 kilograms per cubic meter.

The TVD requirements are obtained by assuming a family of 99 percent synthetic wind profiles obtained from a report entitled "Directional Wind Component Frequency Envelopes, Cape Kennedy, Florida, Atlantic Missile Range" by Orvel E. Smith and Glenn E. Daniels of the Marshall Space Flight Center. An Eastern Test Range (ETR) launch is assumed with a launch azimuth sector of 45° to 115°. TVD requirements are calculated for both pitch and yaw planes. The results presented consist of TVD requirements when no aerodynamic surfaces are used and TVD requirements as a function of fin and canard area. The TVD requirements due to other factors such as thrust misalignment, pitch over, and thrust tailoff (for the SSOPM vehicle) are discussed. The reduction in vehicle bending moments obtainable with canards is also presented. Detailed six degree of freedom trajectory simulation results are presented to verify the approximations used in calculating TVD requirements.

ANALYSIS OF THRUST VECTOR DEFLECTION REQUIREMENTS DUE TO WINDS

Assumptions

The TVD requirements are calculated for two different launch vehicles - the 260-inch solid-SIVB and a large solid launch vehicle (SSOPM) designed to deliver 450 000 kilograms of payload to a 185 kilometers circular orbit. Some of the assumptions and ground rules of the study are listed below.

(1) The thrust and weight data for the 260-inch solid vehicle are taken from reference 1. The data for the SSOPM are based on a preliminary design study conducted at the Lewis Research Center. Some of these data are presented in table I. The three configurations studied are shown in figure 1.

(2) The nominal trajectory for each vehicle was designed at Lewis. Basically, the first (booster) stage was constrained to fly zero angle of attack through the atmosphere after a rapid initial pitchover phase. The upper stages used a steering program generated by the calculus of variations in order to maximize payload capability into a 185 kilometers circular orbit. The magnitude of the initial pitchover maneuver, which determines the amount of trajectory lofting, was allowed to be optimized to maximize payload capability, but with the constraint that the dynamic pressure should not exceed 47 000 newtons per square meter.

(3) Vehicle aerodynamic data (center of pressure and normal force coefficients) were obtained by using analytical techniques developed at Lewis. These techniques are presented in appendix B.

(4) Aerodynamic data for the base fins were taken from a previously mentioned report by Dunn. Canard aerodynamic data comes from the wind tunnel data used for reference 3. A set of either eight fins or four canards was assumed.

(5) An ETR launch was assumed for both vehicles with a launch azimuth sector of 45° to 115°.

(6) Synthetic wind data were used in calculating TVD requirements. The peak velocities used are based on a 99 percent probability of occurrence in the worst monthly period. The wind envelopes are functions of altitude and azimuth heading.

Since most conventional autopilots are designed to fly the nominal pitch program (trimmed) in the presence of disturbances, the TVD requirements quoted herein are based on trim requirements. The results presented in reference 2 show that for the type of vehicle considered herein at least 80 percent of the fully trimmed requirement must be provided for vehicle stability. It is assumed that the vehicle is maintained trimmed up to its maximum TVD capability.

The TVD requirements for a given wind distrubance are calculated by superimposing the wind disturbance on the nominal trajectory and assuming that the trajectory does not drift from the nominal due to the presence of the disturbance. These assumptions lead to a slightly conservative estimate of TVD required because the actual trajectory drifts in a direction which tends to reduce the angle of attack. For the vehicles studied, the drift effect can reduce the TVD requirements by as much as 30 percent as will be shown by detailed results later. The equations used for calculating TVD requirements are presented in appendix C.

The aerodynamic data for the extended Voyager and Apollo configurations of the 260-inch solid vehicle and for SSOPM are presented in figures 2 and 3. Center of pressure (C_p) data are presented in figure 2 and normal force coefficient (C_{N_α}) data in figure 3 as functions of Mach number and angle of attack. The values of C_p and C_{N_α} for angles of attack less than 2° or greater than 10° are assumed to be equal to the corresponding values at 2° and 10°, respectively. The center of pressure is higher on the vehicle for extended Voyager than for Apollo due to the long extended Voyager payload shape. The Mach number, altitude, and dynamic pressure from the nominal trajectories are presented in figures 4 through 6, respectively, as functions of time of flight. The nominal trajectories for the Apollo and extended Voyager configurations of the 260-inch solid vehicle are assumed to be identical as shown in these figures. Since the nominal trajectory is zero angle of attack, the different center of pressure and normal force coefficient data have no effect. A slight difference in axial drag between the two configurations is neglected in the calculation of the nominal trajectory.

Results

Thrust vector deflection requirements. - The TVD requirements for the three configurations are shown in figures 7(a), (b), and (c) for 99 percent winds based on the worst monthly period. Both pitch and yaw plane results are presented. For each plane, the launch azimuth (between 45° and 115°) resulting in the largest TVD requirement is used. The yaw requirement is larger for all three configurations. The deflection profiles shown in figures 7, as well as later figures, correspond to an envelope of maximum deflection requirements for a family of winds rather than to any single wind profile. The synthetic wind profiles consist of low wind velocity regions with a wind spike occurring at some altitude. The height of the spike (maximum wind velocity) is a function of the spike altitude and the wind azimuth. Deflection profiles for two typical synthetic winds are illustrated in figure 7(a). The TVD required at the peak velocity corresponds to a single point on the deflection profile shown in figures 7 as illustrated in figure 7(a). Since the pitch and yaw requirements were obtained for different wind profiles, these requirements should not be added vectorially. Instead, the yaw requirement should be interpreted as essentially the largest total requirement.

Peak TVD requirements tend to occur just prior to maximum dynamic pressure. The winds in the pitch plane are always tail winds because of the launch azimuth sector and the fact that winds tend to blow from the west in the northern hemisphere. The tail winds tend to reduce the relative velocity and dynamic pressure, hence also TVD requirements. Winds in the yaw direction result in increased relative velocity, dynamic pressure, and TVD requirements. In addition, the flight path angle tends to reduce pitch plane TVD requirements as shown in appendix C. The maximum TVD requirements can be seen to be 1.35° and 2.3° for the 260-inch solid vehicle with Apollo and Voyager payloads, respectively. The TVD requirement for SSOPM is 1.17°.

In figure 8, TVD requirements are presented for the three configurations as a function of total base fin area (eight fins) divided by vehicle reference area. It is assumed that the center of pressure of the fins is at the gimbal station on the vehicle and that the angle of attack on the fins is the same as on the vehicle. A 260-inch solid-Voyager vehicle with total fin area ratio of 1.4 is sketched on figure 8(e). The aerodynamic data for the fins are presented in figure 9. The equations used in calculating TVD requirements against fin area are presented in appendix C.

The TVD requirements are presented as a function of total canard area (four canards) in figures 10(a) to (f). The canards are located at 62.4 meters above the gimbal station on the 260-inch solid configurations and at 114.3 meters above the gimbal station on SSOPM. These locations were chosen to place the canards as far forward on the cylindrical protion of the vehicle as possible. This results in minimum canard area (for a given deflection capability) and also minimizes vehicle bending moments, as will be

shown later. The canards are assumed to be rotated to the position which results in maximum normal force, hence minimum required deflection angle. A 260-inch solid-Voyager vehicle with total canard area ratio of 0.9 is sketched on figure 10(e). Canard aerodynamic data is taken from the wind tunnel data used for reference 3 and presented in figure 11.

Several other factors should be considered in selecting the desired canard location. First, the vehicle must be structurally capable of withstanding the loading imposed by the canards. The problem of jettisoning the canards must also be considered. (The canards are jettisoned since they are not useful out of the atmosphere.) Finally, a communications link must be established between the canards and the launch vehicle control system, presumably located on the booster stage. All of these problems are alleviated somewhat when the canard station is lowered on the vehicle.

The selection of the optimum canard location is beyond the scope of this report. However, canard capability for any station location can be easily determined from the data presented. For example, suppose that a canard location of 50 meters above the gimbal station is selected for the 260-inch solid Voyager configuration. The data in table I show that the center of gravity is approximately 23 meters above the gimbal station for all flight times. Thus, the required canard area ratios in figures 10(a) and (e) should be increased by a factor of $(62.4 - 23)/(50 - 23) = 1.46$.

The peaks of figures 8 and 10 are crossplotted on figure 12 to show the TVD required as a function of fin and canard surface area. The TVD requirements presented are for the larger of the pitch and yaw plane requirements. The results presented show that for all configurations and surface areas the canards are more effective in reducing TVD requirements. This is not a surprising result since the canards are movable, whereas the fins are stationary. For the 260-inch solid Apollo vehicle, the TVD required for winds can be reduced to 0.5° either by using base fins with total area of 0.65 times the vehicle base area or by canards of 0.33 times the vehicle base area. However, the added complexity involved in using canards tends to offset the advantage of smaller size. The reduction of bending moments which can be obtained by using canards will be discussed later. If the TVD capability is 1°, then the required area ratios are 0.14 for canard and 0.22 for fins.

For the 260-inch solid Voyager vehicle the results and conclusions are similar. To reduce TVD requirements to 0.5°, base fins of 1.44 or canards of 0.71 area ratio are required. Again, the required fin area is about twice the required canard area. For larger TVD capability, the required fin area decreases much more quickly than the required canard area. For the SSOPM vehicle, the required fin area is always less than twice the required canard area, regardless of TVD capability.

Figure 13 presents TVD requirements for the 260-inch solid-SIVB vehicle with a family of payload shroud densities and shapes. The payload shrouds consist of a conical

nose section and a cylindrical section, such that the product of volume and density yields the required payload weight of 43 000 kilograms. Three different payload shapes are sketched in the figure. The TVD requirements are calculated for a flight time of 60 seconds for the yaw plane. This set of conditions resulted in maximum TVD requirements for both the Apollo and Voyager configurations of the 260-inch solid vehicle. The largest semi-vertex angle considered is 40°, and the smallest is such that the conical section gives the required payload weight with no cylindrical section.

Results are presented for payload densities of 31.9, 70.2, and 319 kilograms per cubic meter. The results show that for payload densities greater than 70.2 kilograms per cubic meter, the TVD required for winds is less than 2.4° for the payload shapes considered.

Vehicle bending moments. - Figures 14(a), (b), and (c) show the possible reduction in vehicle bending moments which can be obtained if canards are used. The results are presented for the extended Voyager configuration at a flight time of 60 seconds and a 99 percent yaw wind. A flight time of 60 seconds is illuatrated because bending moments are near maximum at that time. Similar results would be obtained for other flight conditions or vehicles.

In figure 14(a), bending moments are shown along the vehicle for various canard stations with a canard area ratio of 0.6. In each case, the canards are deflected to obtain maximum normal force, and the residual moment is supplied by TVD. The no canard, all TVC case is also presented for comparison. The results presented for comparison. The results presented clearly show that bending moments are reduced as the canard station is moved forward. The most critical region for bending moments is likely to be between the 260-inch solid-SIVB interstage (station 1450) and the SIVB-payload interstage (station 2100). In order to reduce the moments at station 2100, the canards must be located above this station on the payload.

The canards in figure 14(b) have been set at station 2600 above the gimbal station. This location has been chosen as being as far forward as possible on the cylindrical portion of the vehicle. Bending moments are shown as a function of canard size with TVD used as required to maintain trim conditions. The required TVD is about zero for a canard area ratio of 1.0 which also results in minimum bending moments. Actually, bending moments can be further reduced by oversizing the canards and using negative TVD to maintain trim conditions until the bending moment becomes negative.

In figure 14(c), the canard size is varied at each station such that the canards supply all of the required moment, and no TVD is used. The canard size decreases as the station increases, and the best canard station both for size and bending moments is again seen to be as far forward on the vehicle as is practical.

Detailed Simulation Results

In order to establish the validity of the approximations used in generating the results presented, detailed computer simulation results were obtained for the three configurations studied. A six degree of freedom computer simulation was used, and the trajectory was simulated by trimming the vehicle to the nominal pitch program when wind disturbances were present. Each configuration was flown with two winds, one real and one synthetic. The real wind velocity profile is presented in figure 15. The real wind azimuth was approximately 280°. The synthetic wind profile is illustrated in figure 16. This wind has a 99 percent peak velocity and shear, the peak occurring at an altitude of 12.2 kilometers. Figures 17 to 19 show the pitch and yaw deflection profiles obtained for the two wind profiles and three vehicle configurations. The deflection profiles obtained by using the approximate methods employed herein are also presented for comparison. The synthetic wind was simulated either as a pitch or yaw wind for the three vehicles. Therefore only one thrust vector deflection profile is presented for each vehicle for the synthetic wind. As shown by these figures, the approximate results are always conservative but never by more than 30 percent (fig. 19(b), real wind, SSOPM vehicle). For high shear winds, the agreement is very good. The real wind profile simulated had the highest and broadest peak of the 100 wind profiles presented in a report entitled "FPS-16 Radar/Jimsphere Wind Data Measured at the Eastern Test Range" by James R. Scoggins and Michael Susko of the Marshall Space Flight Center. Although no statistical number can be attached to this wind, it is felt to be extremely conservative, especially for broadness of peak, which is the factor which tends to degrade the accuracy of the approximations used herein.

ADDITIONAL THRUST VECTOR DEFLECTION REQUIREMENTS

It should be noted that, in addition to the TVD requirements for winds, additional thrust vector deflection is required to compensate for such factors as thrust misalinement, pitch program, and vehicle dispersions. The TVD required to compensate for these effects is summarized in table II along with the TVD required for winds. The values for thrust misalignment and thrust and weight dispersions were taken from reference 1 and were assumed to be the same for all configurations studied. The TVD required for pitchover was obtained from six degree of freedom computer simulations with a conventional autopilot design. The total TVD requirement was calculated by adding the root-sum-square of the wind gusts, thrust misalinement, and thrust and weight dispersions to the steady state wind requirement. The wind requirement was added, rather than root-sum-squared, since the wind profile is known at the time of launch. Since the TVD required for pitchover and for winds occur at different times during the flight, the pitch-

over requirement does not contribute to the overall TVD requirement. Other effects, such as launch release transients and ground winds, have been studied and were found to be small compared to thrust misalinement.

If aerodynamic control surfaces are used, TVD must still be supplied to control the vehicle early in flight when these surfaces are ineffective. Simulations have shown that canards can supply enough torque to handle pitchover requirements but not thrust misalinement. If base fins are used, TVD must be supplied for pitchover, thrust misalignment, and flight control and stability.

An additional effect, which must be considered, is the TVD required for thrust unbalance during tailoff for multiengine solid rocket configurations. This effect applies to the SSOPM vehicle which has a first stage consisting of seven 260-inch (6.61 m) solid rocket motors. A base view of these motors is shown in figure 20. A thrust unbalance results in a torque about the center of gravity, since the thrust vectors of the six outside engines do not pass through the center of gravity. This torque must be cancelled or at least kept within reasonable bounds; otherwise, the vehicle will rotate away from the nominal flight path. The resulting angle of attack may result in problems during upper stage separation, as well as aerodynamic heating.

In order to calculate the TVD required to maintain control during tailoff, nominal and dispersed thrust tailoff data must be known. The thrust decay profiles used herein were taken from reference 4 and are presented in figure 21. The data presented reflect Titan III C flight experience, as well as available test data. The data are applied to SSOPM by taking them to represent percent of maximum thrust for each motor.

Results are calculated for three different motor decay modes. In two of the cases, six motors are assumed to follow the nominal decay curve, while the seventh (an outside motor) is either 3σ low (decay mode I) or 3σ high (decay mode II). For the third decay mode, five motors are assumed to be nominal while two opposite outside motors are 3σ high and 3σ low, respectively. This decay mode is somewhat more conservative than the usual 3σ design criteria.

The TVD required to maintain the nominal flight path (trim) throughout decay is shown on figure 22 for the three decay modes. For decay modes II and III, more than 6° of TVD is required to trim the vehicle near separation. Separation is assumed to occur when the thrust acceleration has decreased to 1.0 m/sec^2, as in reference 4.

Since the 6° requirement occurs only in the last few seconds before separation, it was decided to assume various TVD capabilities less than or equal to that required for all other effects (1.49°, table II). The vehicle will then be trimmed until the TVD capability is exceeded. The resulting attitude and attitude rate errors can be calculated by using the data in table I.

Attitude and attitude rate errors at separation are shown in table III for the three decay modes and for TVD capability of 0.5°, 1.0°, and 1.5°. The largest errors occur

for decay mode III, as expected. Reasonable limits on attitude and attitude rate errors are about 3^{o} and 2^{o} per second, respectively. With these limits, the attitude (approximately equal to angle of attack) at second stage startup will not exceed 10^{o} for a three second delay from separation to upper stage startup. For angles of attack greater than about 10^{o}, aerodynamic heating could become important, even at the altitude (about 65 km) the vehicle has reached at separation. The results shown in table III indicate that 0.5^{o} or at most 1.0^{o} of TVD is adequate, depending on the degree of conservation used in selecting the 3σ design tailoff mode.

CONCLUDING REMARKS

Thrust vector deflection requirements have been calculated for anticipated wind profiles by assuming a trim autopilot. In order to provide trim conditions in the high wind velocity region for 99 percent wind profiles, thrust vector deflection angles of 1.35^{o} and 2.3^{o} are required for the 260-inch solid-SIVB launch vehicle with Apollo and Voyager payloads, respectively. For the large solid-solid-OPM launch vehicle, it was found that 1.17^{o} was required. For all the configurations studied in this report, approximately 0.35^{o} is required (in addition to the thrust vector deflection required for winds) for effects such as thrust misalinement and vehicle thrust and weight dispersions. The pitch-over requirement is 0.5^{o}, but this is already available and does not add to the total requirement. The effects of thrust unbalance during tailoff were studied for the SSOPM vehicle. It was found that about one degree of TVD is sufficient to maintain an acceptable degree of control.

Thrust vector requirements were found to depend critically on payload density and shape for the 260-inch solid vehicle. However, for payload densities greater than 70.2 kilograms per cubic meter, the thrust vector requirements did not exceed those of the 260-inch solid-Voyager vehicle.

It was found that the thrust vector requirements could be reduced by using either stationary base fins or movable canards. For the 260-inch solid-Voyager vehicle, the thrust vector deflection requirements for steady state winds can be reduced to 0.5^{o} by using base fins or canards, with a total fin or canard area of 1.44 or 0.71 times the vehicle reference area, respectively. For the 260-inch solid-Apollo and SSOPM vehicles, the required aerodynamic surface areas are even smaller.

The results presented show that maximum bending moments are reduced by a factor of five (25×10^{6} N-m to 5×10^{6} N-m) for the 260-inch solid-Voyager vehicle with a canard

area ratio of 1.0. Also, the bending moments at the SIVB-payload interstage are reduced from 11×10^6 to 4×10^6 N-m.

Lewis Research Center,
National Aeronautics and Space Administration,
Cleveland, Ohio, March 28, 1968,
125-17-05-01-22.

APPENDIX A

SYMBOLS

A	vehicle area, m^2
a, b	constants defined in appendix C, sec^{-1}
C_{D_c}	cross flow drag coefficient
C_G	center of gravity, m above gimbal station
C_N	normal force coefficient
C_{N_α}	normal force coefficient per angle of attack, rad^{-1}
$C_{N_{\alpha_c}}$	normal force coefficient per angle of attack for cone, rad^{-1}
$C_{N_{\alpha_s}}$	loading per angle of attack at cone-cylinder junction, rad^{-1}
C_p	center of pressure, m above gimbal station
D	local diameter, m
D_{ref}	reference diameter, m
d	constant defined in appendix C, sec^{-2}
$\frac{dC_N}{dX}$	aerodynamic normal force distribution, m^{-1}
F_A	axial drag, N
F_c	canard normal force, N
g	gravitational constant, m/sec^2
I	moment of inertia, $N\text{-}m\text{-}sec^2$
K	decrease in loading along cylinder
L_s	length of cylinder, m
m	mass, kg
N	normal force per angle of attack, N/rad
Q	dynamic pressure, N/m^2
S	area, m^2
S_{ref}	vehicle reference area $S_{ref} = \frac{\pi D_{ref}^2}{4}$; m^2
s	Laplace operator, $(sec)^{-1}$
T	thrust, N
v	velocity, m/sec
X	length along the vehicle, m
α	angle of attack, rad
γ	flight path angle, rad
δ	deflection angle, rad
δ_{max}	maximum deflection angle, rad
θ	vehicle pitch attitude, rad
μ_α	vehicle aerodynamic parameter (eq. (C2)), sec^{-2}
μ_c	vehicle control parameter, (eq. (C2)), sec^{-2}
ρ	atmospheric density, kg/m^3
τ	conical semi-vertex angle, rad

Subscripts:

c	canards
cf	cross flow
f	base fins

n	nominal
p	potential flow
rel	relative
w	wind

Superscript:

derivative with respect to time

APPENDIX B

AERODYNAMIC NORMAL FORCE CALCULATION

The simplified analysis for calculating the aerodynamic normal forces used in this study is similar to the analyses of references 5 to 7. The aerodynamic normal force is separated into a normal force due to the potential flow and a cross flow normal force which accounts for the viscosity of the air flowing over the vehicle. The analysis for this study assumes that the potential normal force component is linear with the vehicle angle of attack in radians, and the cross flow normal force component varies with the square of the sine of the angle of attack.

$$C_N = C_{N_p} \alpha + C_{N_{cf}} \sin^2 \alpha \tag{B1}$$

The vehicle is made up of conical and cylindrical components, each having a particular aerodynamic normal force distribution associated with it. The aerodynamic normal force distribution of the complete vehicle is obtained by joining the distributions of each vehicle component. This distribution is integrated over panel lengths along the vehicle and multiplied by the product of the vehicle reference area and the dynamic pressure to obtain discrete normal forces for control and bending moment calculations.

Conical Body

The aerodynamic normal force coefficient distribution for a conical body is:

$$\frac{dC_N}{dX} = \frac{dC_{N_p}}{dX} \alpha + \frac{dC_{N_{cf}}}{dX} \sin^2 \alpha \tag{B2}$$

where the potential component is a function of the cross sectional area and a normal force coefficient for a sharp cone. The cone normal force coefficient is constant since the pressure distribution is assumed to be constant over the surface of the cone. Thus, the potential component is:

$$\frac{dC_{N_p}}{dX} = \frac{C_{N_{\alpha_c}}}{S_{ref}} \frac{dA}{dX}$$

where

$$A = \frac{\pi D^2}{4}$$

$$D = 2X \tan \tau$$

Therefore:

$$\frac{dC_{N_p}}{dX} = \left[\frac{C_{N_{\alpha_c}}}{S_{ref}} \, 2\pi \tan^2 \tau \right] X$$

The value of $C_{N_{\alpha_c}}$ can be obtained from references 8 and 9 for sharp cones and is assumed to approach the slender body value of two at subsonic speeds.

The cross flow component is a function of the planform area of the conical body and a cross flow drag coefficient which is assumed constant over the length of the body. Therefore, the cross flow component of the normal force coefficient distribution is:

$$\frac{dC_{N_{cf}}}{dX} = \frac{C_{D_c}}{S_{ref}} \frac{dA}{dX}$$

where

$$A = \frac{1}{2} XD = X^2 \tan \tau$$

Thus:

$$\frac{dC_{N_{cf}}}{dX} = \left[\frac{2C_{D_c}}{S_{ref}} \tan \tau \right] X$$

For the range of Mach numbers and angles of attack considered, C_{D_c} has a value of 0.80 from reference 5. Combining the potential and cross flow terms for the normal force coefficient distribution produces:

$$\frac{dC_N}{dX} = \left[\frac{2\pi C_{N_{\alpha_c}} \alpha \tan^2 \tau}{S_{ref}} + \frac{2C_{D_c} \tan \tau \sin^2 \alpha}{S_{ref}} \right] X \qquad \text{(B3)}$$

where α is in radians.

For a sharp cone the value of X is zero at the vertex and is equal to the length of the cone at the base. A conical frustum is a cone with a smaller cone removed from the front; therefore, X begins at the front of the frustum with a value equal to the length of the removed cone. This process ignores any two-dimensional flow effects at the front of the frustum and any other effects caused by any body preceding the frustum. For the case of a blunted nose on a vehicle, the first value of X is taken at the tip of the nose cap and has a value equal to the distance from the cone vertex to the nose cap. This assumption does not completely account for the effect of the normal force of the nose cap or any flow effects due to bluntness. These effects would be small for small bluntness ratios.

Cylindrical Body

The aerodynamic normal force coefficient distribution for a cylindrical body located behind a conical body is:

$$\frac{dC_N}{dX} = \frac{dC_{N_p}}{dX} \alpha + \frac{dC_{N_{cf}}}{dX} \sin^2 \alpha \qquad \text{(B4)}$$

The potential flow component is a function of the cross sectional area and an aerodynamic normal force for the cylinder which accounts for the flow expansion at the cone-cylinder junction. The potential normal force for a cylinder consists of a loading at the cone-cylinder junction and a decrease in loading along the cylinder as indicated in reference 7. For this analysis, the loading at the junction from reference 7 is assumed to be the loading per unit diameter. The normal force coefficient due to potential flow over the cylinder is:

$$C_{N_p} = \frac{C_{N_{\alpha_s}}}{D} \frac{A}{S_{ref}} \int_0^{L_s} K \, dX$$

Thus, the distributed normal force coefficient for the constant cross sectional area of the cylinder is:

$$\frac{dC_{N_p}}{dX} = \frac{C_{N_{\alpha_s}}}{S_{ref}} \frac{\pi D}{4} K$$

where the coefficient $C_{N_{\alpha_s}}$ is the loading at the cone-cylinder junction and approaches zero for Mach number equal to zero. The parameter K is the decrease in loading along the cylinder. The value of K varies from one at the cone-cylinder junction to a very small value at the base of the cylinder for long cylindrical bodies. Both the parameter K and the data for $C_{N_{\alpha_s}}$ are taken from reference 7.

The cross flow component of cylindrical bodies is also a function of the planform area and a constant cross flow drag coefficient as was the case for the conical body. Therefore, the normal force coefficient distribution due to cross flow is:

$$\frac{dC_{N_{cf}}}{dX} = \frac{C_{D_c}}{S_{ref}} \frac{dA}{dX}$$

where

$$A = XD$$

$$\frac{dC_{N_{cf}}}{dX} = \frac{C_{D_c}}{S_{ref}} D$$

Combining the potential and cross flow components for the distribution of the cylindrical body yields:

$$\frac{dC_N}{dX} = \frac{C_{N_{\alpha_s}}}{S_{ref}} \alpha \frac{\pi D}{4} K + \frac{C_{D_c}}{S_{ref}} D \sin^2 \alpha \qquad \text{(B5)}$$

where α is in radians.

The normal force coefficient parameters for the conical and cylindrical components can be adjusted as wind tunnel data of various vehicle configurations become available. This analysis does not consider ogives or configurations having boattails or rearward facing steps on the cylinder. Also, the analysis does not take into account the effects due

to protuberances, boundary layer effects, or whether the flow is attached or separated other than through the input from analytical and wind tunnel tests of launch vehicles. Increasing the accuracy of this analysis could affect the magnitude of the control requirements and the vehicle bending moment but would not change the qualitative conclusions of this report.

APPENDIX C

EQUATIONS USED IN CALCULATING DEFLECTION REQUIREMENTS

The vehicle equations of motion in the pitch plane are:

$$\left.\begin{aligned}
\ddot{\theta} &= \mu_c \sin \delta + \mu_\alpha \alpha \\
\alpha &= \theta - \gamma - \alpha_w \\
\dot{\gamma} &= \frac{1}{mv}\left[T \sin (\theta - \gamma + \delta) - F_A \sin (\theta - \gamma) + N\alpha \cos (\theta - \gamma) - mg \cos \gamma\right] \\
\dot{v} &= \frac{1}{m}\left[T \cos (\theta - \gamma + \delta) - F_A \cos (\theta - \gamma) - N\alpha \sin (\theta - \gamma) - mg \sin \gamma\right] \\
\sin \alpha_w &= \frac{v_w}{v_{rel}} \sin \gamma
\end{aligned}\right\} \quad (C1)$$

where

$$\left.\begin{aligned}
N &= QS_{ref}C_{N_\alpha} \\
\mu_c &= \frac{TC_G}{I} \\
\mu_\alpha &= \frac{N}{I}(C_p - C_G) \\
Q &= \frac{1}{2}\rho V_{rel}^2
\end{aligned}\right\} \quad (C2)$$

All symbols are defined in appendix A, and some are illustrated in figure 23. Equations (C1) may be applied to the yaw plane by setting g = 0. If equations (C1) are linearized about the nominal values, the floowing equations are obtained.

$$
\left.
\begin{aligned}
\dot{\theta} &= \mu_c \delta + \mu_\alpha \alpha \\
\alpha &= \theta - \gamma - \alpha_w \\
\dot{\gamma} &= \frac{1}{m v_n}\left[N\alpha + mg \sin \gamma_n \gamma + T(\theta - \gamma + \delta) - F_A(\theta - \gamma)\right] + g \frac{\cos \gamma_n}{v_n^2} v \\
\dot{v} &= -g \cos \gamma_n \gamma \\
\sin \alpha_w &= \frac{v_w}{v_{rel}} \sin \gamma_n
\end{aligned}
\right\} \qquad \text{(C3)}
$$

In equation (C3) and in the equations that follow, the unsubscripted state variables refer to the linearized variables. A zero angle of attack, zero wind nominal trajectory has been assumed in equation (C3); that is,

$$\theta_n = \gamma_n$$

$$\alpha_n = \alpha_{w,n} = 0$$

In addition, it has been assumed that $\delta_n \approx 0$. For the yaw plane, $\gamma_n = \theta_n = 90^o$.

The linearized trajectory is assumed to be trimmed through the wind disturbance so that

$$\theta = 0; \qquad \delta = -\frac{\mu_\alpha}{\mu_c} \qquad \text{(C4)}$$

Combining equations (C3) and (C4), switching to LaPlace notation, and solving for α in terms of α_w results in

$$\alpha = -\left(\frac{s^2 + as + d}{s^2 + bs + d}\right)\alpha_w \qquad \text{(C5)}$$

where

$$a = \frac{T - F_A - mg \sin \gamma_n}{mv_n}$$

$$b = \frac{T\left(1 + \frac{\mu_\alpha}{\mu_c}\right) + N - F_A - mg \sin \gamma_n}{mv_n}$$

$$d = \frac{g^2 \cos^2 \gamma_n}{v_n^2}$$

The constants a, b and d are vehicle and trajectory dependent. Both a and b are nearly equal early in flight (because N is small), and both become small as v_n increases. The d is always small since γ_n is nearly 90^o early in flight and v_n increases later. Therefore, it may be assumed that

$$\alpha \approx - \alpha_w \tag{C6}$$

This is equivalent to assuming a zero drift trajectory, or $\gamma = 0$. In reference 2, as well as in the six degree of freedom simulations presented in this report, it is shown that the drift effect for the configurations studied amounts to no more than 30 percent and tends to reduce the angle of attack. Thus, the no-drift assumption leads to a conservative estimate for deflection requirements.

By using equations (C2) and (C6), equation (C4) becomes:

$$\delta = \frac{N(C_p - C_G)}{TC_G} \frac{v_w}{v_{rel}} \sin \gamma_n \tag{C7}$$

Equation (C7) is used for calculating trim deflection requirements in this report.

Deflection Requirements With Fins

If stationary base fins are added to the vehicle, the TVD required is reduced since the fins supply some of the torque necessary to cancel the aerodynamic moment. The torque balance equation is

$$TC_G\delta + N(C_p - C_G)\alpha + N_f(C_{p,f} - C_G)\alpha = 0 \tag{C8}$$

Here it has been assumed that the angle of attack on the fins is the same as on the vehicle. The fin normal force is given by:

$$N_f = QS_f C_{N_{\alpha_f}} \tag{C9}$$

By using equations (C2) and (C9), equation (C8) becomes:

$$\delta = \frac{QS_{ref}V_w \sin\gamma_n}{TC_G V_{rel}} \left[C_{N_\alpha}(C_p - C_G) - C_{N_{\alpha_f}}(C_G - C_{p,f}) \frac{S_f}{S_{ref}} \right] \tag{C10}$$

Deflection Requirements for Canards

The canards are assumed to be deflected to the position resulting in maximum normal force, which is a function of angle of attack on the vehicle. This procedure results in the lowest possible TVD requirement. The torque balance equation is

$$TC_G + N(C_p - C_G)\alpha + F_c(C_{p,c} - C_G) = 0$$

or

$$\delta = \frac{N(C_p - C_G)\alpha_w - F_c(C_{p,c} - C_G)}{TC_G}$$

where

$$F_c = QS_c C_{N_c}$$

REFERENCES

1. Dawson, R. P.: Saturn IB Improvement Study (Solid First Stage), Phase II, Final Detailed Report. Rep. SM-51896, vol. II, Douglas Aircraft Co. (NASA CR-77129), Mar. 30, 1966.

2. Borsody, Janos; and Teren, Fred: Stability Analysis and Minimum Thrust Vector Control Requirements of Booster Vehicles During Atmospheric Flight, NASA TN D-4593, 1968.

3. Cubbison, Robert W.; Davidson, Kenneth I.; Turk, Raymond A.; and Alexis, Everett C.: Effect of Canards in Reducing Launch Vehicle Flight loads. NASA TN D-4125, 1967.

4. Dawson, R. P.; Meyers, J. F.; and Goodwin, A. J.: Use of Large Solid Motors in Booster Applications. Volume 2: 156-9n. Vol. 2, Douglas Aircraft Co. (NASA CR-91594), Aug. 30, 1967.

5. Allen, H. Julian; and Perkins, Edward W.: A Study of Effects of Viscosity on Flow Over Slender Inclined Bodies of Revolution. NACA Rep. 1048, 1951.

6. Kelly, Howard R.: The Estimation of Normal-Force, Drag, and Pitching-Moment Coefficients for Blunt-Based Bodies of Revolution at Large Angles of Attack. J. Aeron. Sci., vol. 21, no. 8, Aug. 1954, pp. 549-555, 565.

7. Phythian, J. E.; and Dommett, R. L.: Semi-Empirical Methods of Estimating Forces on Bodies at Supersonic Speeds. J. Roy. Aeron. Soc., vol. 62, no. 571, July 1958, pp. 520-524.

8. Sims, Joseph L.: Tables for Supersonic Flow Around Right Circular Cones at Small Angle of Attack. NASA SP-3007, 1964.

9. Staff of Ames Research Center: Equations, Tables, and Charts for Compressible Flow. NACA Rep. 1135, 1953.

TABLE I. - VEHICLE DATA

(a) Thrust and center of gravity data

Time after liftoff, sec	Center of gravity (Height above gimbal station), m		Thrust, N	
	260-inch solid vehicle	SSOPM	260-inch solid vehicle	SSOPM
20	22.4	45.1	0.265×10^{8}	0.294×10^{9}
25	22.5	45.4	.272	.296
30	22.6	45.7	.279	.298
35	22.7	46.0	.296	.300
40	22.8	46.3	.270	.302
45	22.9	46.6	.253	.305
50	23.0	46.9	.236	.308
55	23.2	47.4	.238	.311
60	23.3	47.7	.242	.314
65	23.4	48.1	.244	.317
70	23.6	48.6	.252	.320
75	23.8	49.1	.268	.323
80	24.1	49.7	.284	.326
85	24.3	50.2	.298	.328
90	24.6	50.9	.313	.329
95	----	51.7	---------	.330
100	----	52.5	---------	.331
105	----	53.4	---------	.332

(b) Other vehicle data

	260-inch solid vehicle	SSOPM
Vacuum thrust, N		
First stage	0.313×10^{8}	0.332×10^{9}
Upper stage	0.911×10^{5}	0.8×10^{8}
Vacuum specific impulse, sec		
First stage	265	265
Upper stage	426	271
Launch weight, kg	0.188×10^{7}	0.248×10^{8}
Orbital payload capability, kg	43 000	450 000
Variables for tailoff calculations		
Moment of inertia, $kg\text{-}m^2$	---------	0.375×10^{10}
Center of gravity, m	---------	70.5

TABLE II. - THRUST-VECTOR DEFLECTION

ANGLE REQUIREMENTS

Parameter	Variation	Apollo	Voyager	SSOPM
		Deflection angle, deg		
1. Steady stage winds	99 percent	1.35	2.30	1.17
2. Wind gusts	3σ	.15	.26	.13
3. Thrust misalinement	3σ	.25	.25	.25
4. Thrust and weights	3σ	.15	.15	.15
5. Pitch program	maximum	.50	.50	.50
[a]Total		1.68	2.69	1.49

[a]Total consists of item 1 plus root sum square of items 2, 3, and 4.

TABLE III. - ATTITUDE AND ATTITUDE-RATE ERRORS

DUE TO UNEQUAL SOLID ROCKET MOTOR

TAILOFF OF SSOPM VEHICLE

Maximum available deflection angle, deg	[a]Decay mode					
	I	II	III	I	II	III
	Attitude error, deg			Attitude rate error, deg/sec		
0.5	1.3	3.2	10.2	0.6	0.9	3.5
1.0	0	.3	2.3	0	.5	1.5
1.5	0	.1	1.2	0	.2	.9

[a]Decay mode: I, 6 motors nominal, 1 outside motor 3σ low; II, 6 motors nominal, 1 outside motor 3σ high; and III, 5 motors nominal, 1 outside motor 3σ low, opposite outside motor 3σ high.

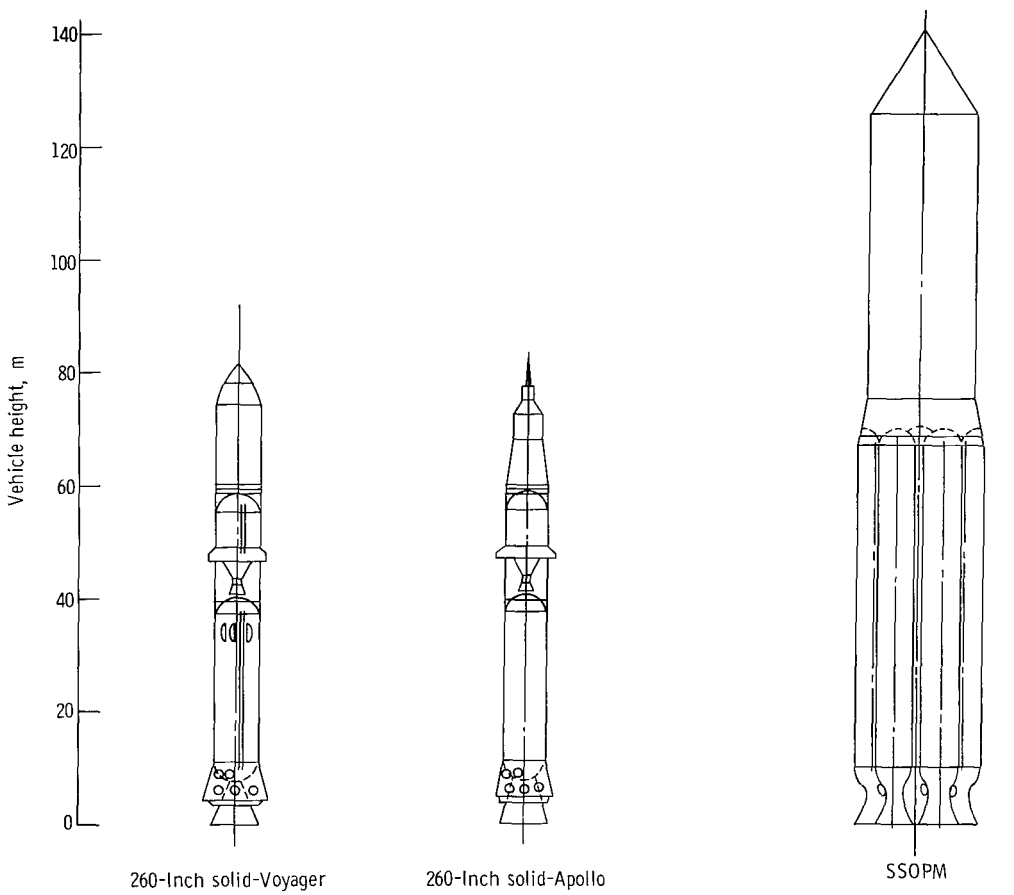

260-Inch solid-Voyager

Reference diameter, 6.59 meter; reference area, 34.1 square meter.

260-Inch solid-Apollo

Reference diameter, 6.59 meter; reference area, 34.1 square meter.

SSOPM

Reference diameter, 21.6 meter; reference area, 366 square meter.

Figure 1. - Vehicle definition.

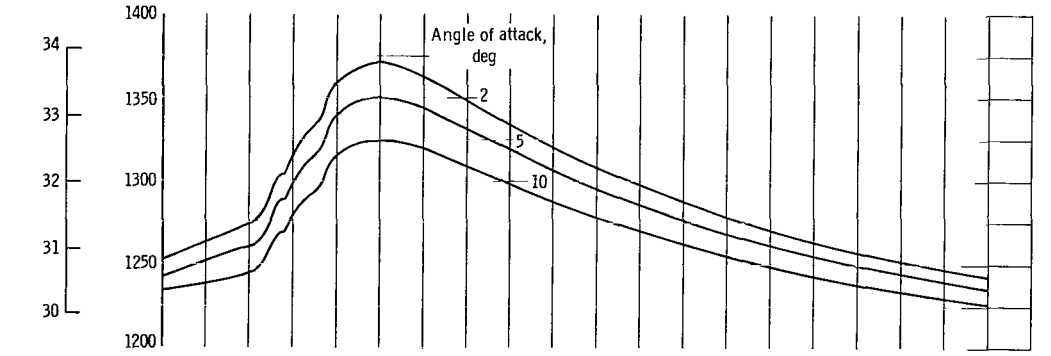

(a) 260-Inch solid-Apollo vehicle.

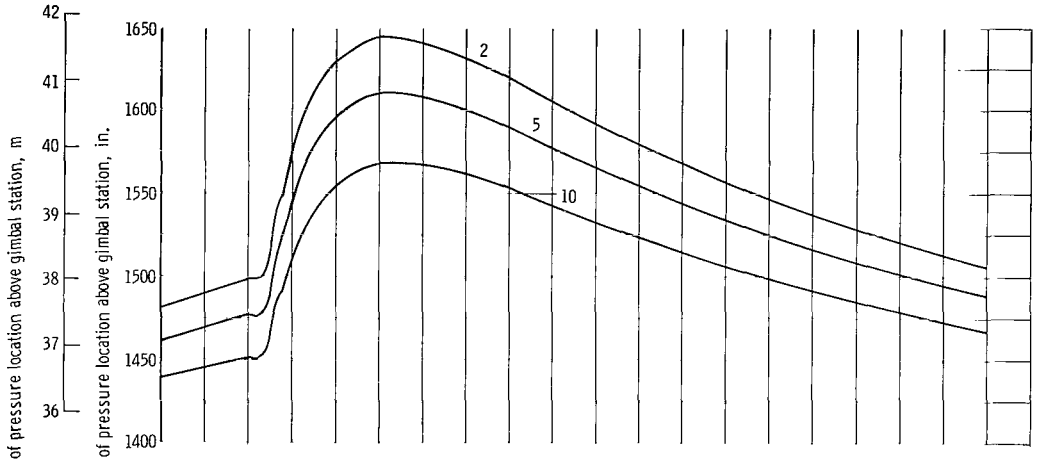

(b) 260-Inch solid-Voyager vehicle.

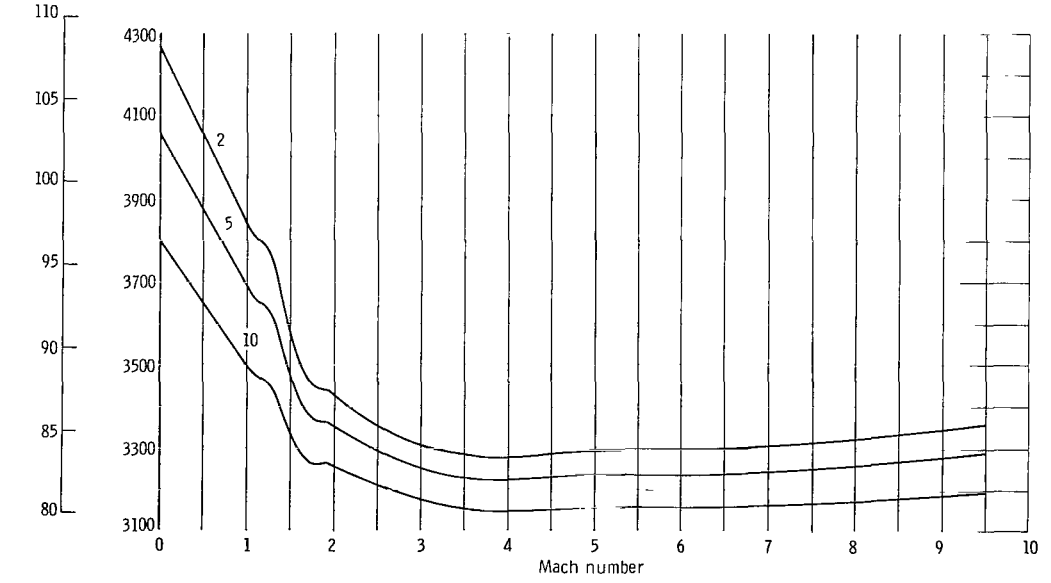

(c) SSOPM vehicle.

Figure 2. - Center of pressure data.

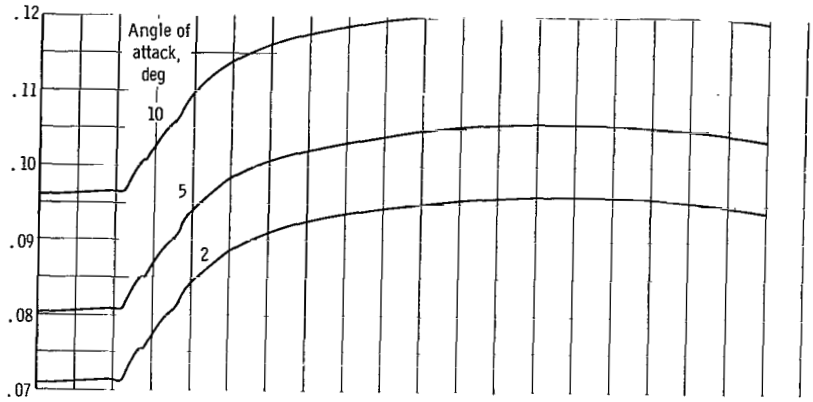

(a) 260-Inch solid-Apollo vehicle.

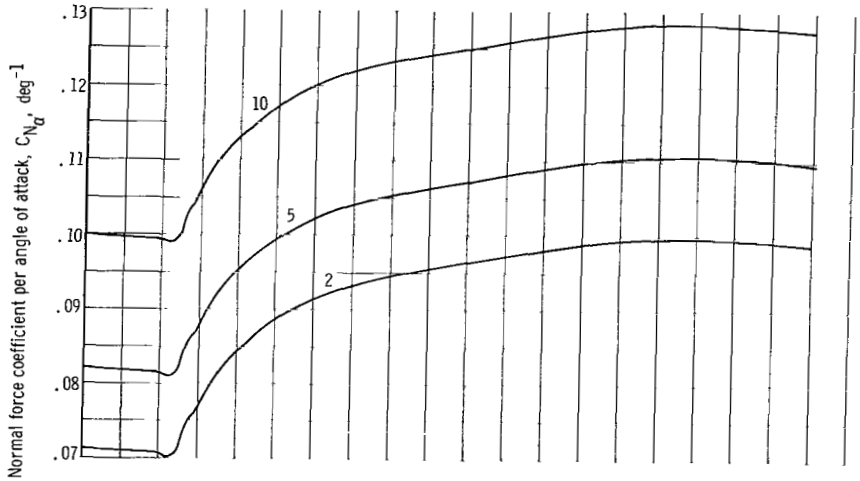

(b) 260-Inch solid-Voyager vehicle.

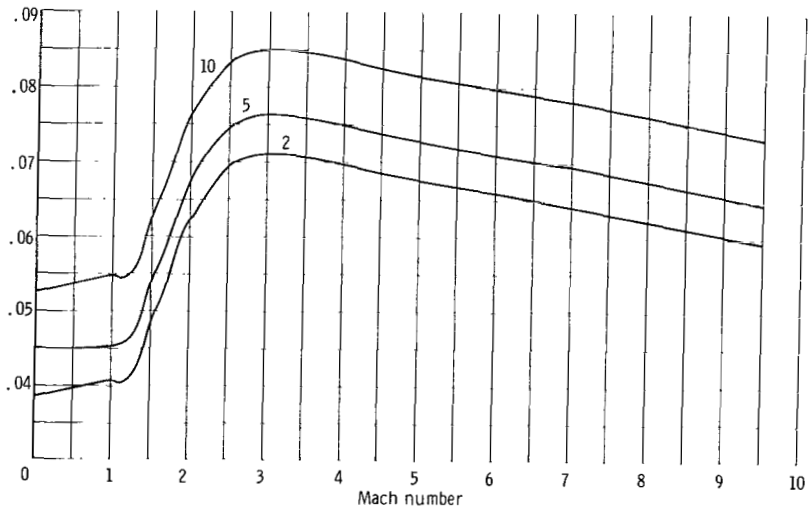

(c) SSOPM vehicle.

Figure 3. - Normal force coefficient data.

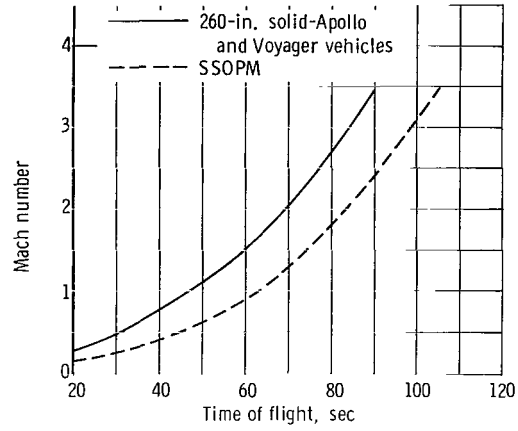

Figure 4. - Nominal Mach number profiles.

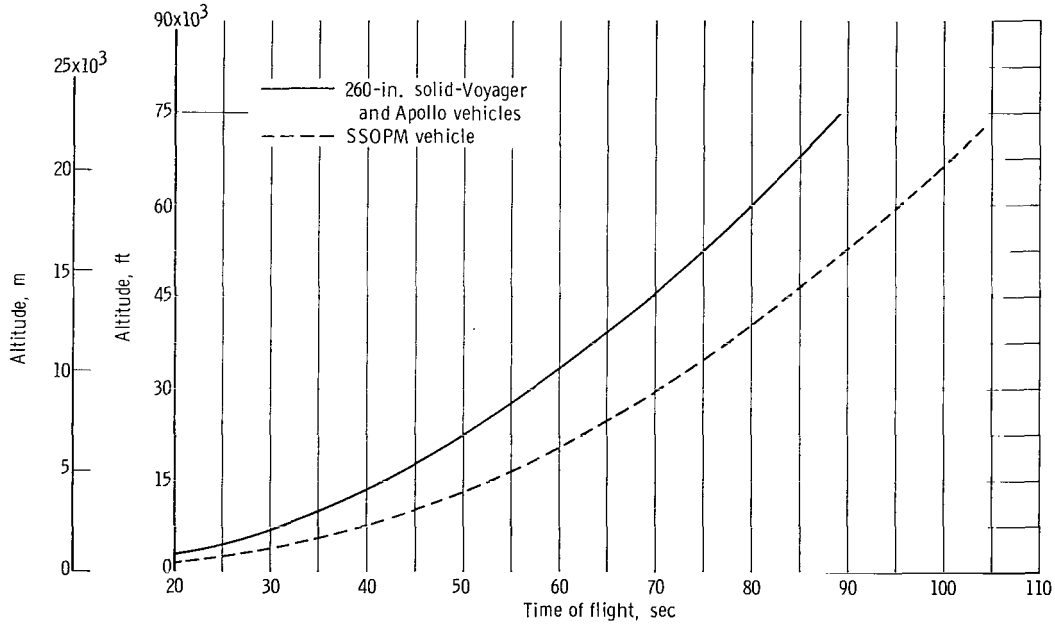

Figure 5. - Nominal altitude profiles.

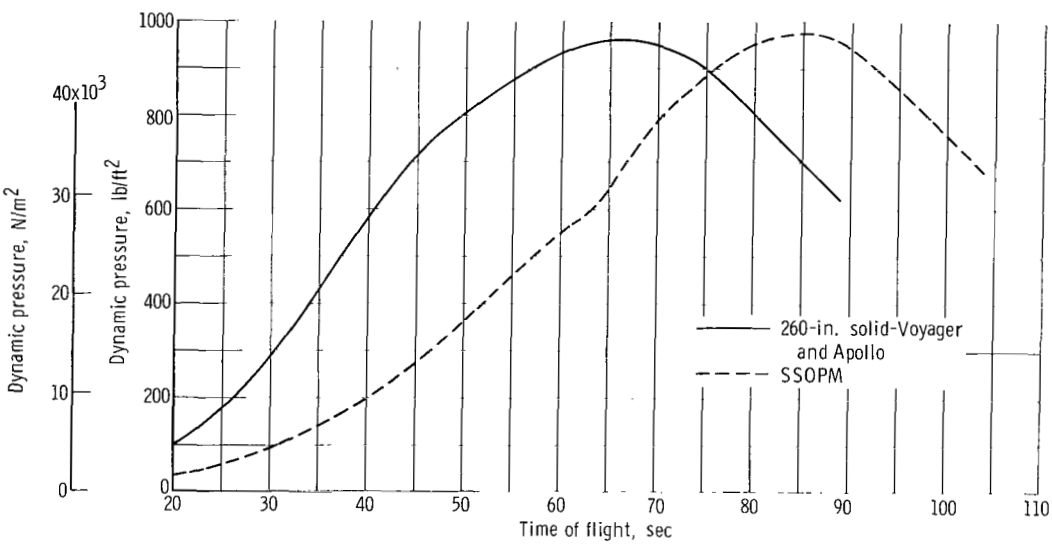

Figure 6. - Nominal dynamic pressure profiles.

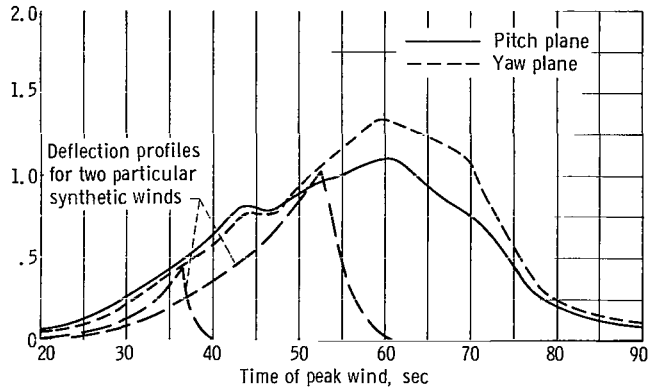

(a) 260-Inch solid-Apollo vehicle.

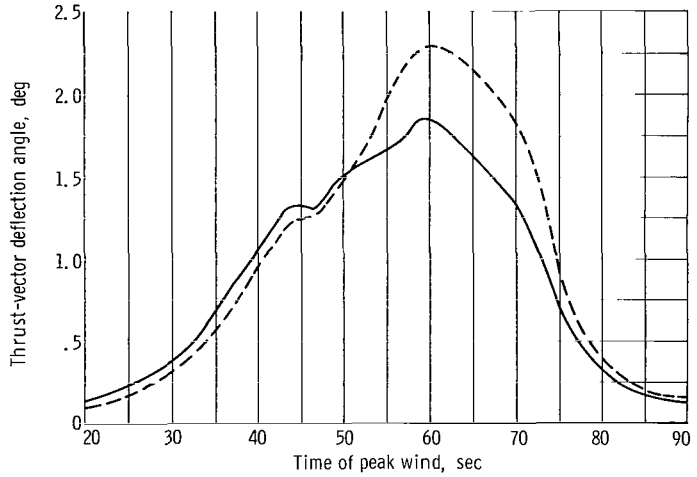

(b) 260-Inch solid-Voyager vehicle.

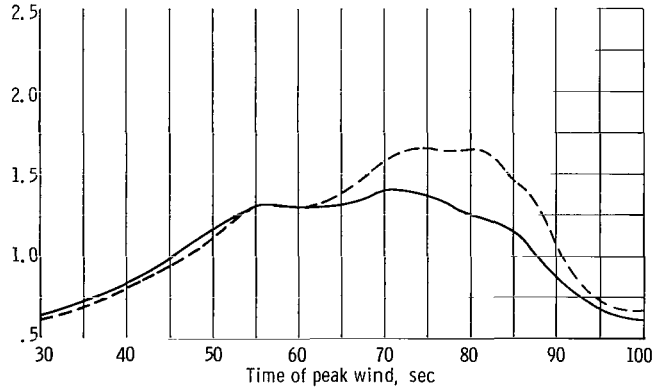

(c) SSOPM vehicle.

Figure 7. - Pitch and yaw deflection requirements for family of 99-percent synthetic wind profiles.

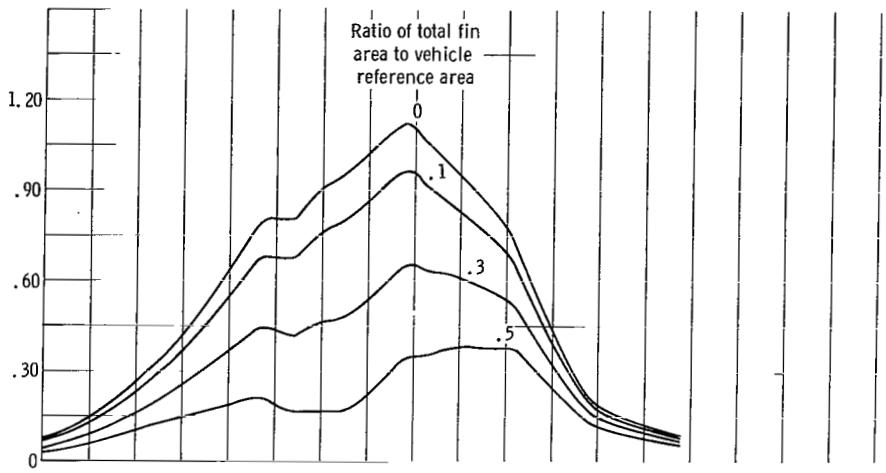

(a) 260-Inch solid-Apollo launch vehicle. Pitch plane.

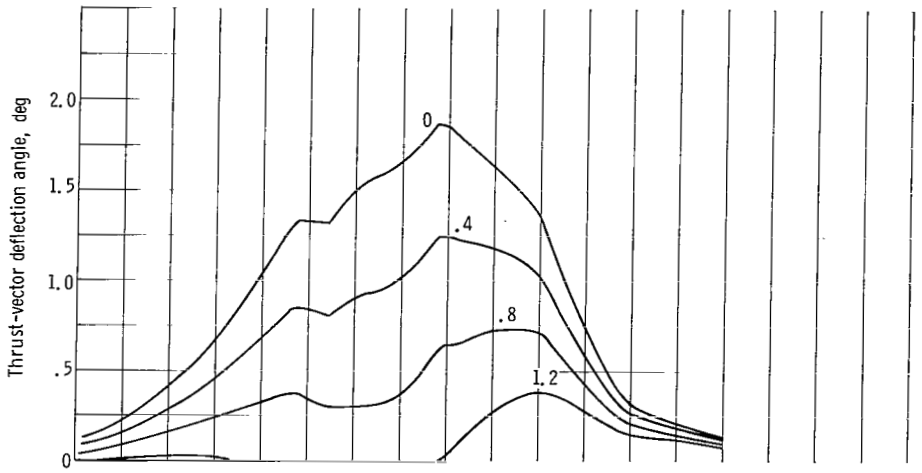

(b) 260-Inch solid-Voyager vehicle. Pitch plane.

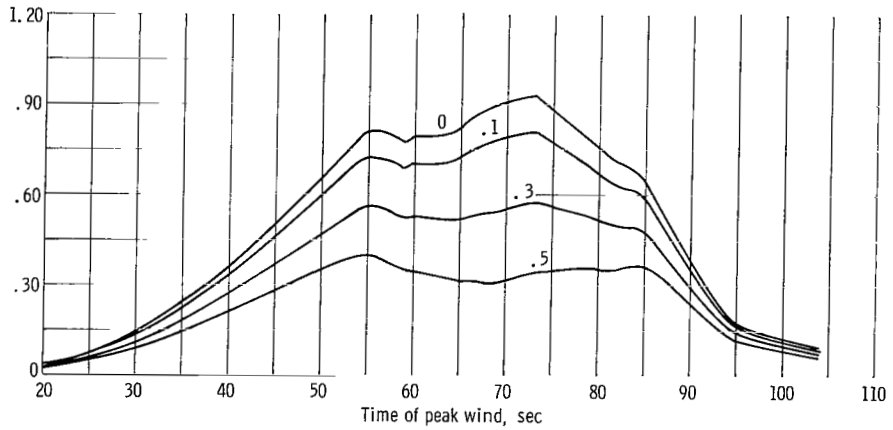

(c) SSOPM vehicle. Pitch plane.

Figure 8. - Deflection requirements for various fin areas.

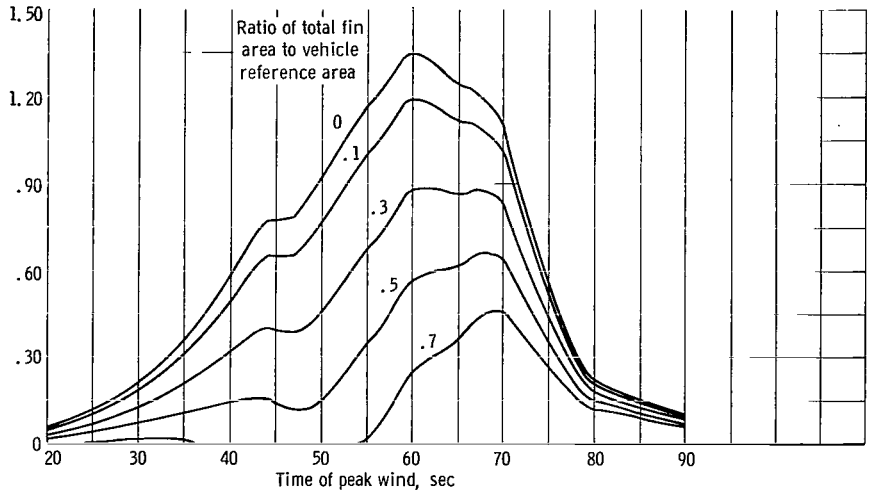

(d) 260-Inch solid-Apollo vehicle. Yaw plane.

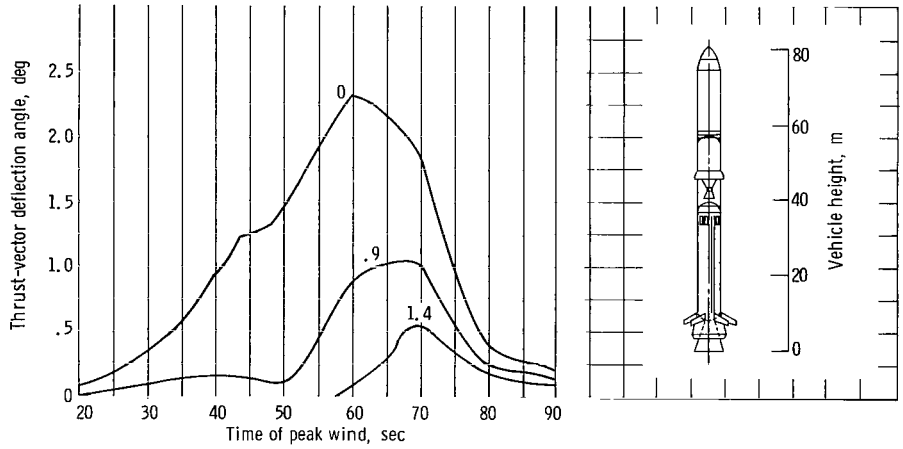

(e) 260-Inch solid-Voyager vehicle. Yaw plane. Ratio of total fin area to vehicle reference area on illustration, 1.4.

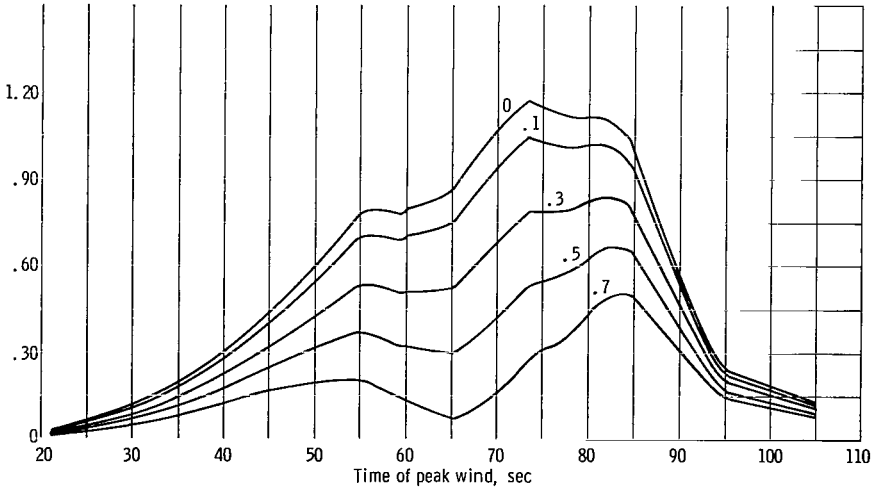

(f) SSOPM vehicle. Yaw plane.

Figure 8. - Concluded.

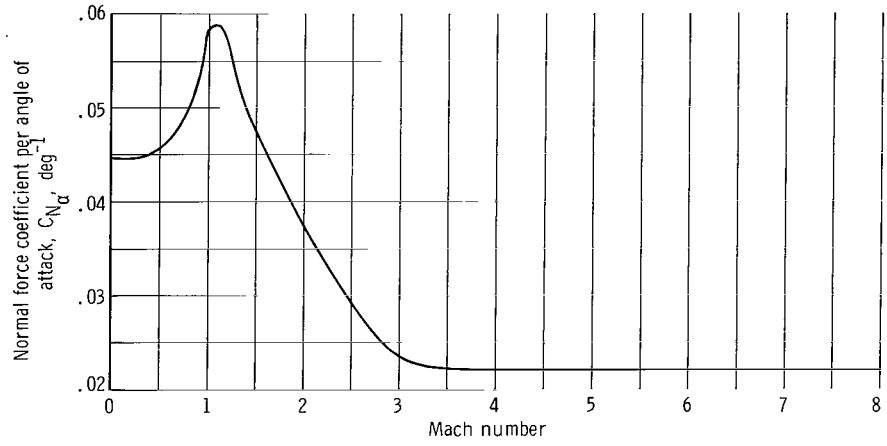

Figure 9. - Base fin aerodynamic data based on total area of eight fins.

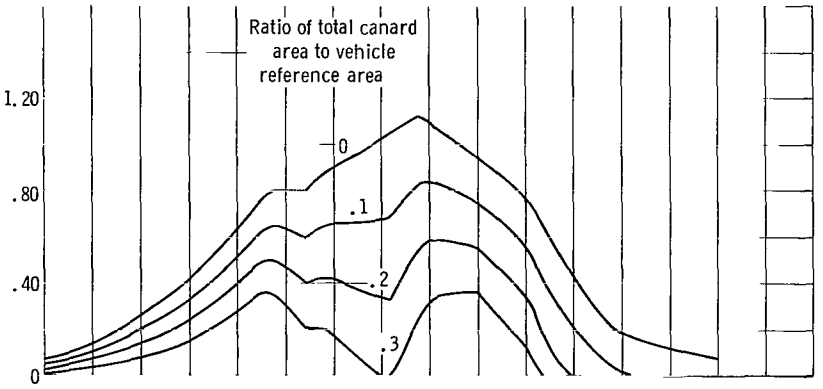

(a) 260-Inch solid-Apollo vehicle. Pitch plane.

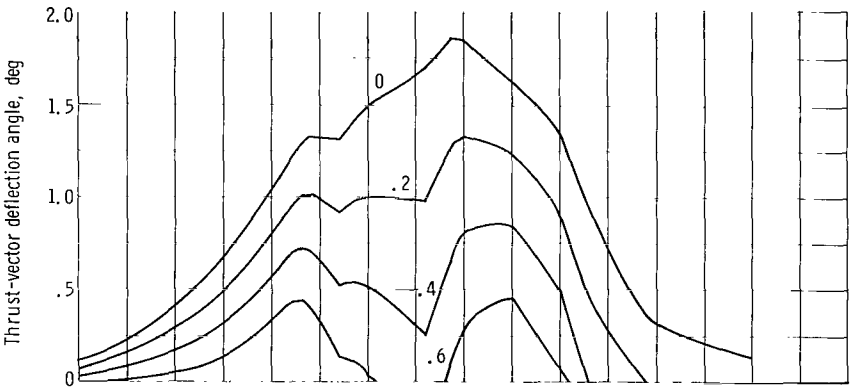

(b) 260-Inch solid-Voyager vehicle. Pitch plane.

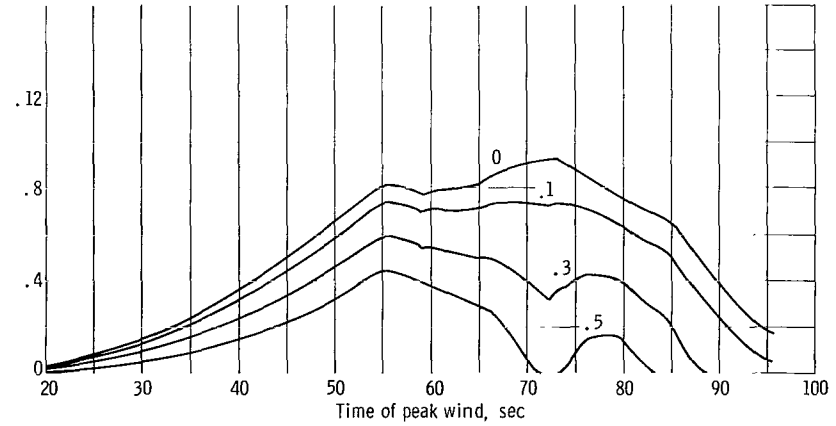

(c) SSOPM vehicle. Pitch plane.

Figure 10. - Deflection requirements for various canard areas.

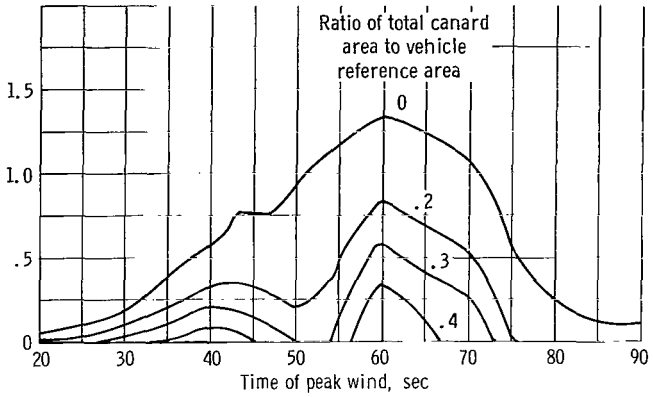

(d) 260-inch solid-Apollo vehicle. Yaw plane.

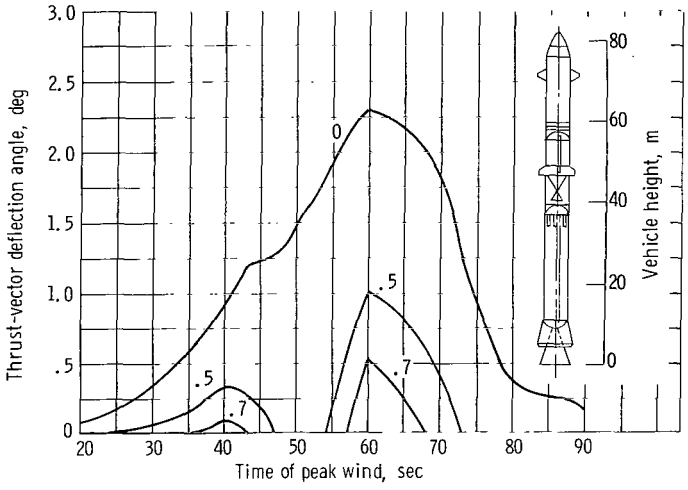

(e) 260-inch solid-Voyager vehicle. Yaw plane. Ratio of total canard area to vehicle reference area on illustration, 0.9.

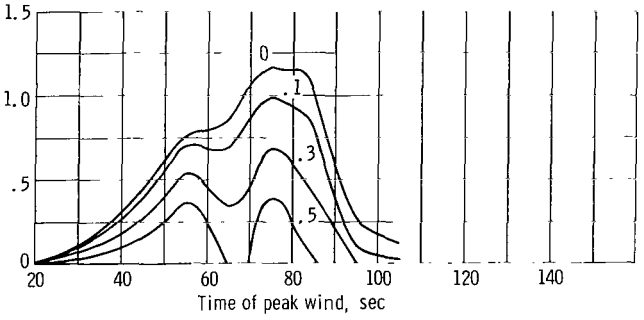

(f) SSOPM vehicle. Yaw plane.

Figure 10. - Concluded.

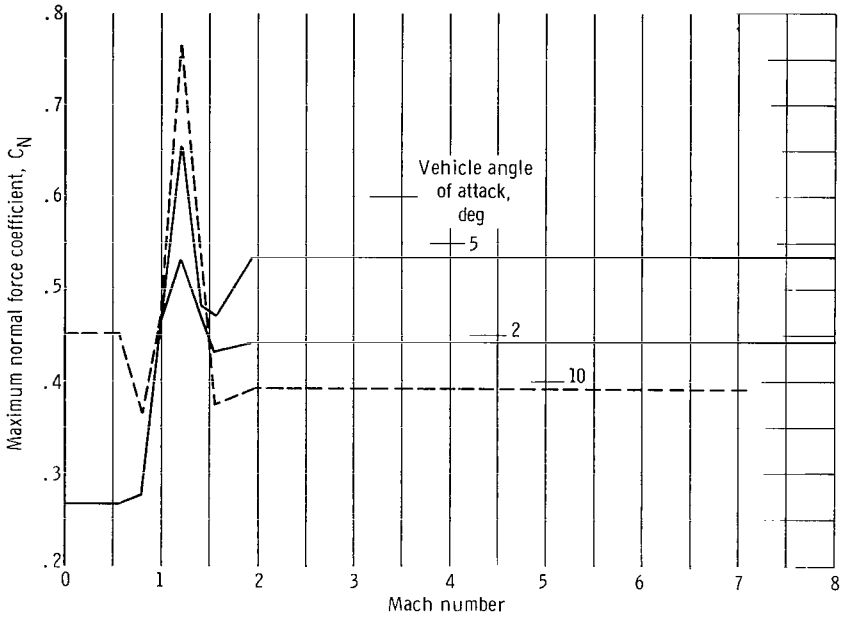

Figure 11. - Canard aerodynamic data based on total area of four canards.

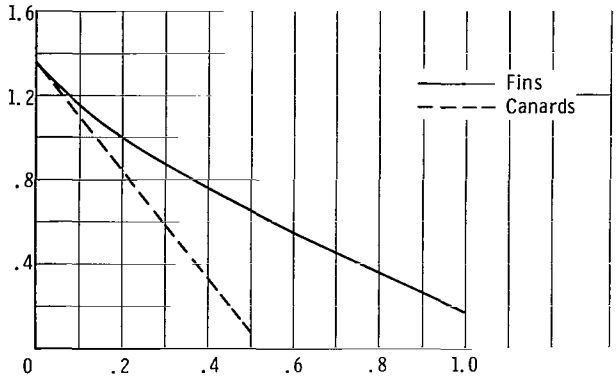

(a) 260 inch solid-Apollo vehicle.

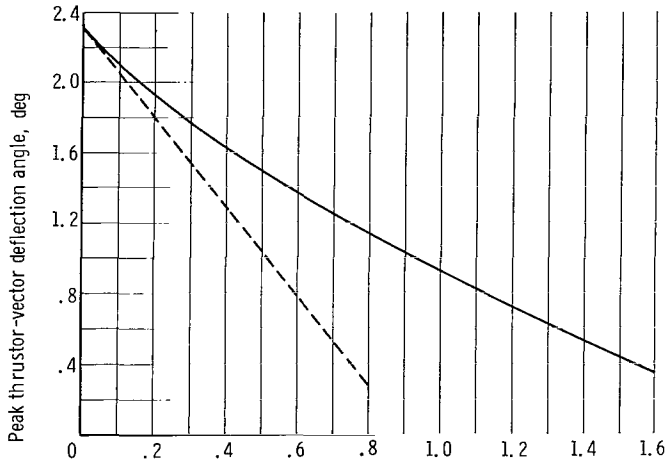

(b) 260 Inch solid-Voyager vehicle.

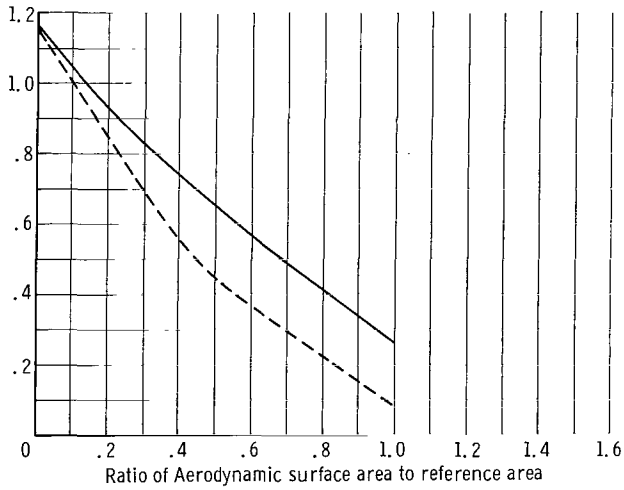

(c) SSOPM vehicle.

Figure 12. - TVC requirements against aerodynamic surface area.

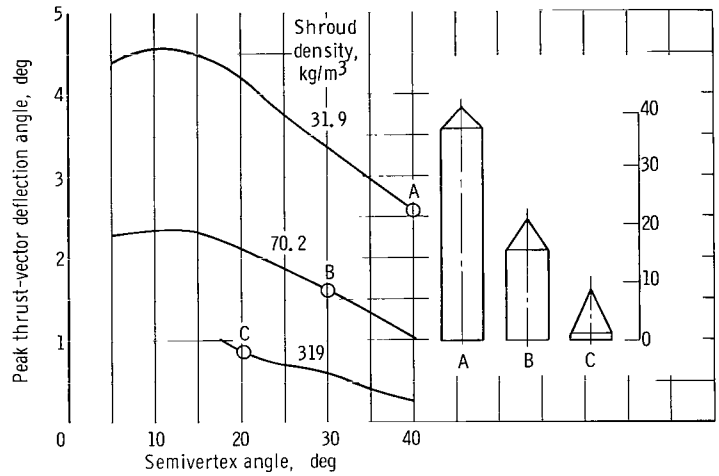

Figure 13. - Deflection requirements against shroud density and shape. 260-Inch solid-SIVB launch vehicle. Payload weight, 43 000 kilograms.

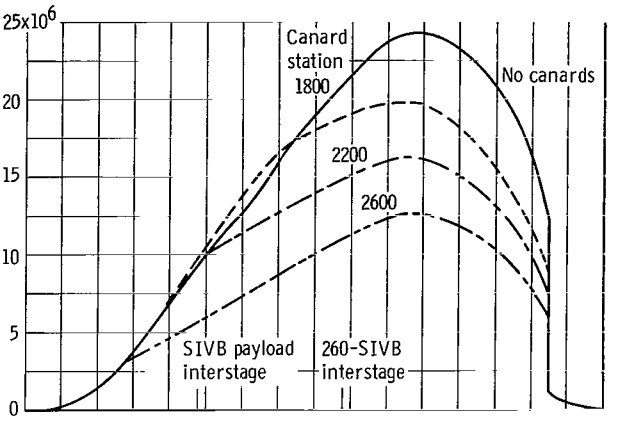

(a) Effect of canard location. Ratio of total canard area to vehicle reference area, 0.6.

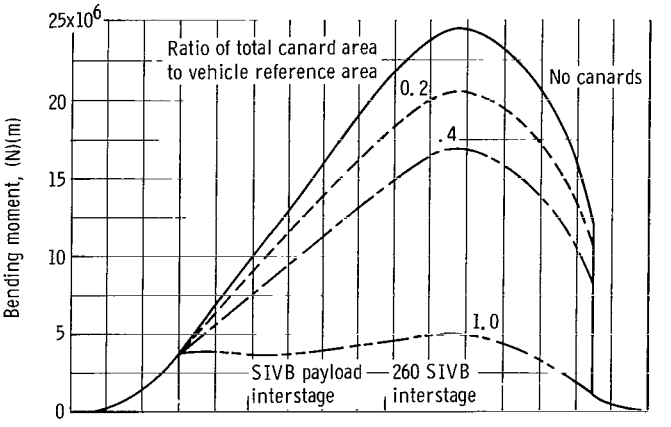

(b) Effect of canard size. Canard station, 2600.

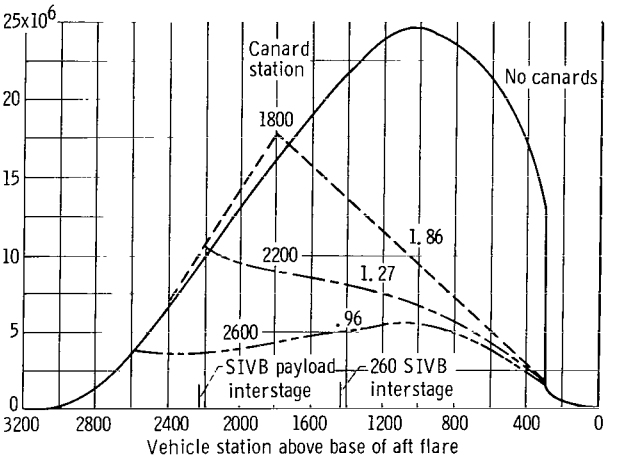

(c) Effect of reducing thrust vector deflection requirement to zero by various combinations of canard size and location.

Figure 14. - Bending moments for 260-inch solid-Voyager vehicle. Mach number, 1.5; angle of attack, 9°; dynamic pressure, 45 600 newtons per square meter.

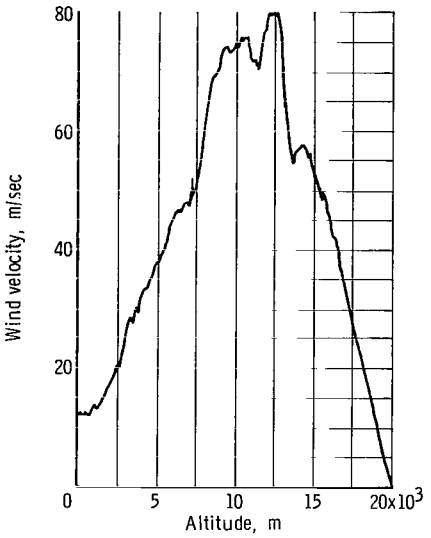

Figure 15. - Real wind velocity profile.

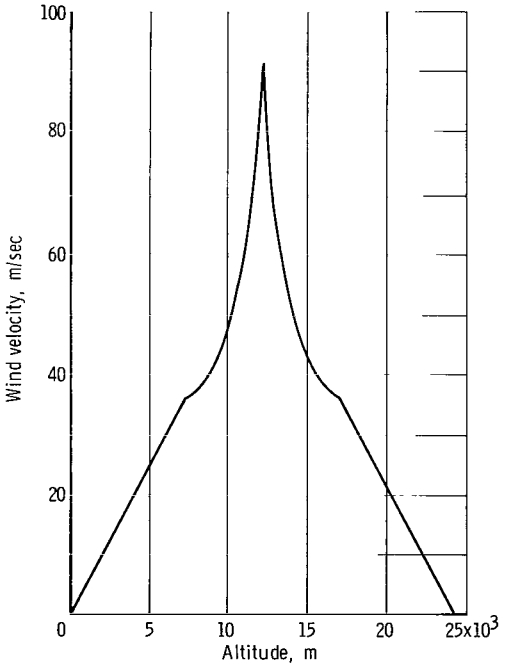

Figure 16. - 99-Percent synthetic wind velocity profile.

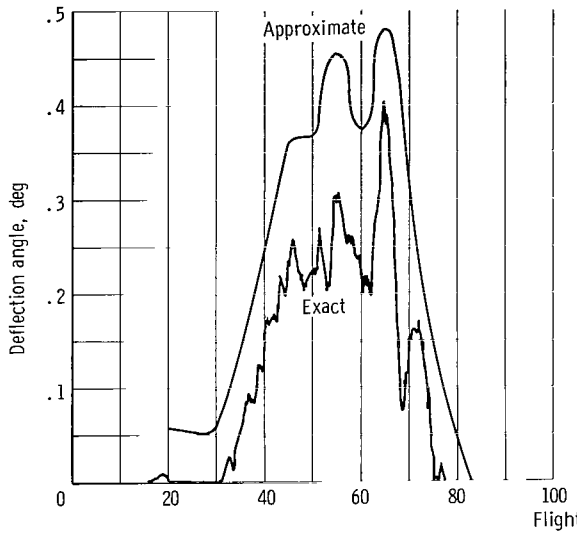

(a) Pitch plane; real wind.

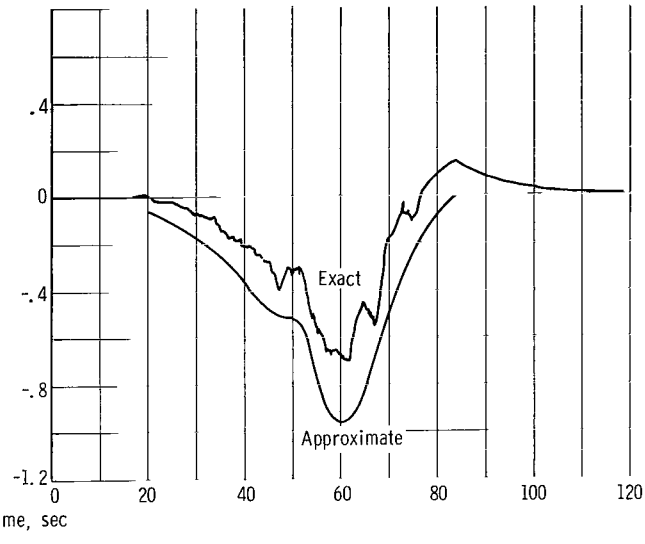

(b) Yaw plane; real wind.

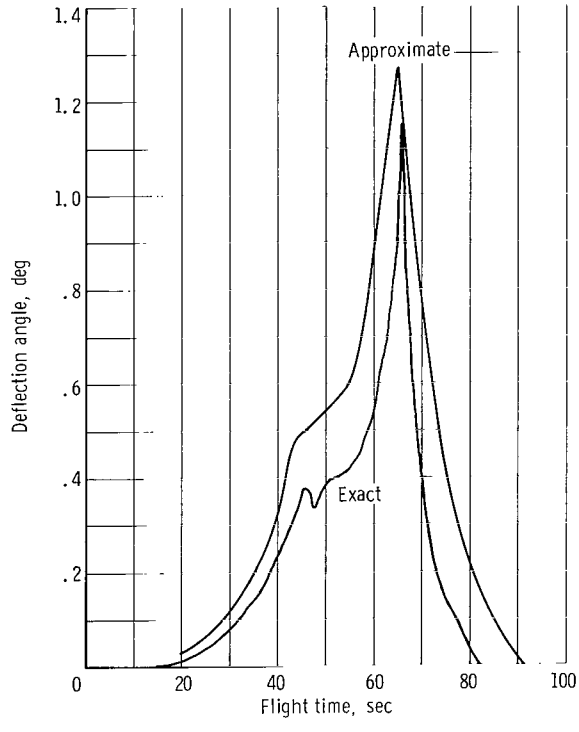

(c) Yaw plane, synthetic wind; wind azimuth, 135°.

Figure 17. - Deflection requirements for 260-inch solid-Apollo vehicle.

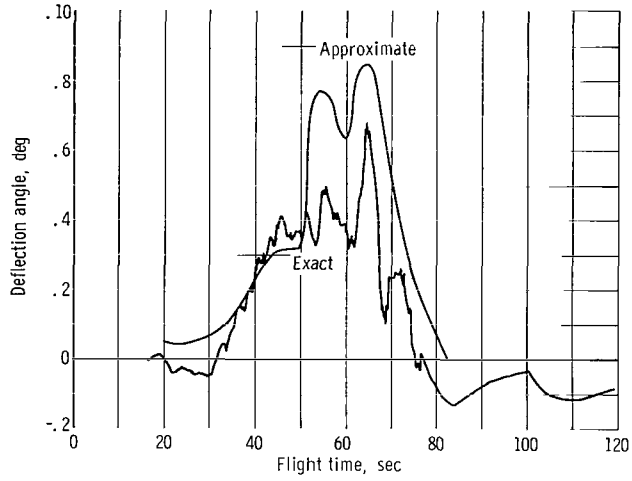

(a) Pitch plane; real wind.

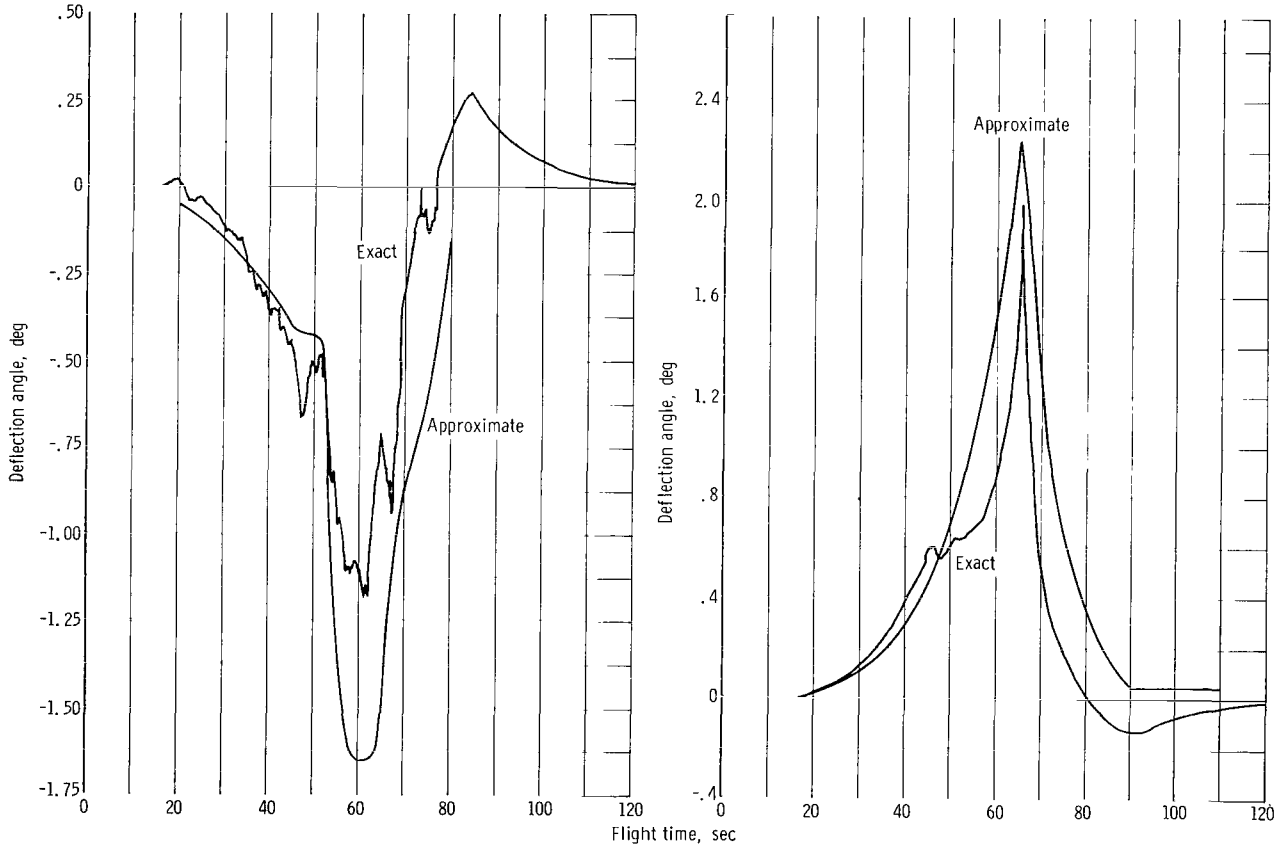

(b) Yaw plane; real wind.

(c) Yaw plane, synthetic wind; wind azimuth, 135°.

Figure 18. - Deflection requirements for 260-inch solid-Voyager vehicle.

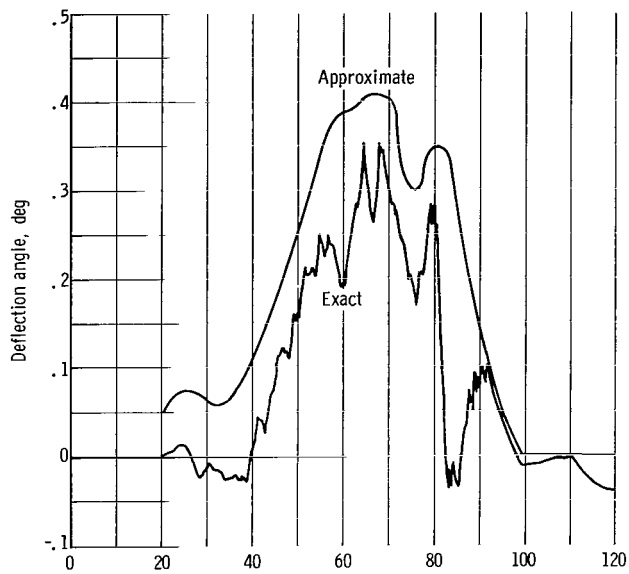

(a) Pitch plane; real wind.

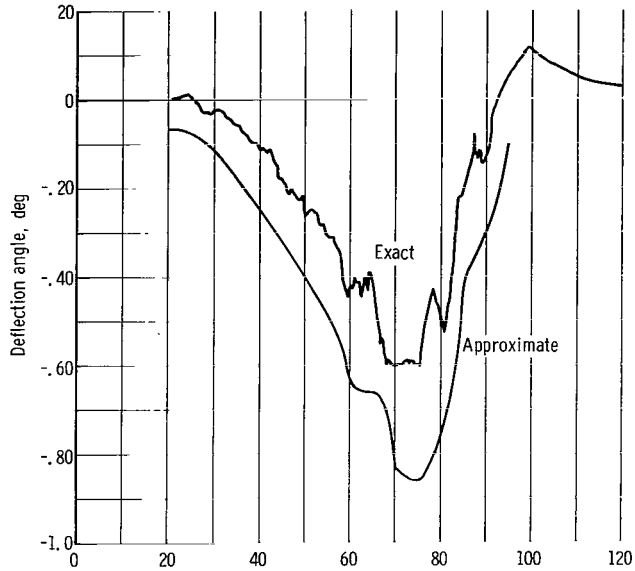

(b) Yaw plane; real wind.

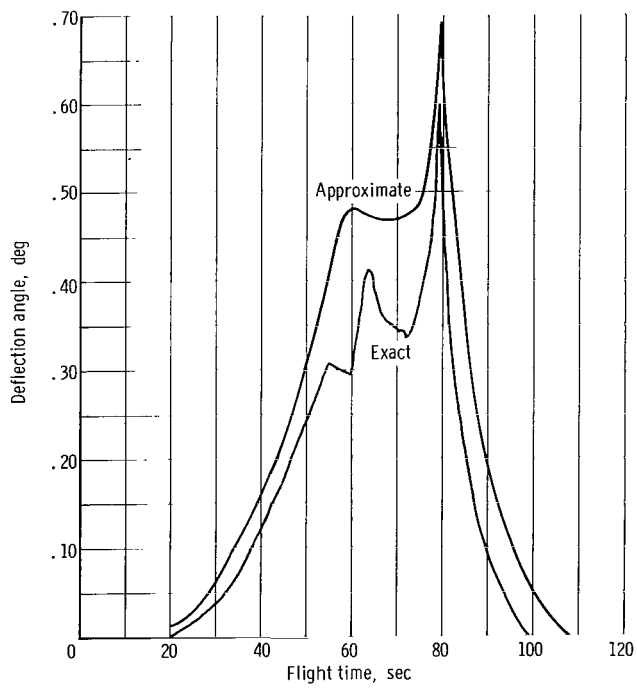

(c) Pitch plane; synthetic wind; wind azimuth, 225°.

Figure 19. - Deflection requirements for SSOPM vehicle.

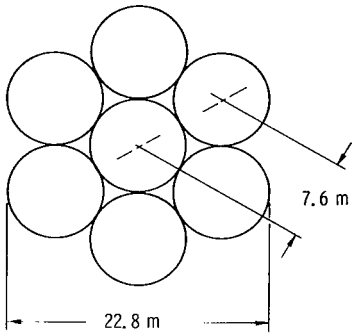

Figure 20. - Bottom view of SSOPM engines with seven 260-inch (660-cm) solid motors.

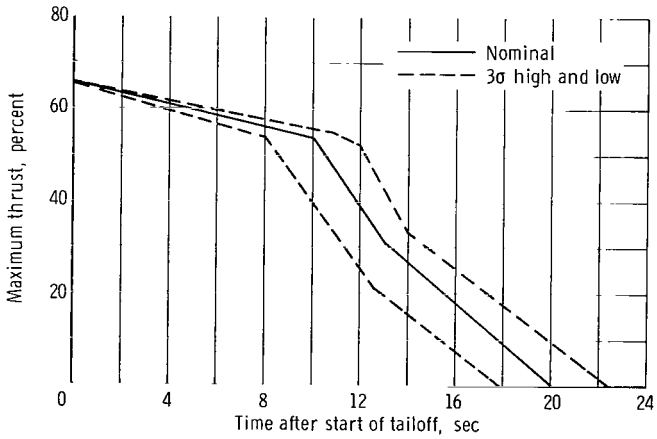

Figure 21. - Solid rocket motor tailoff.

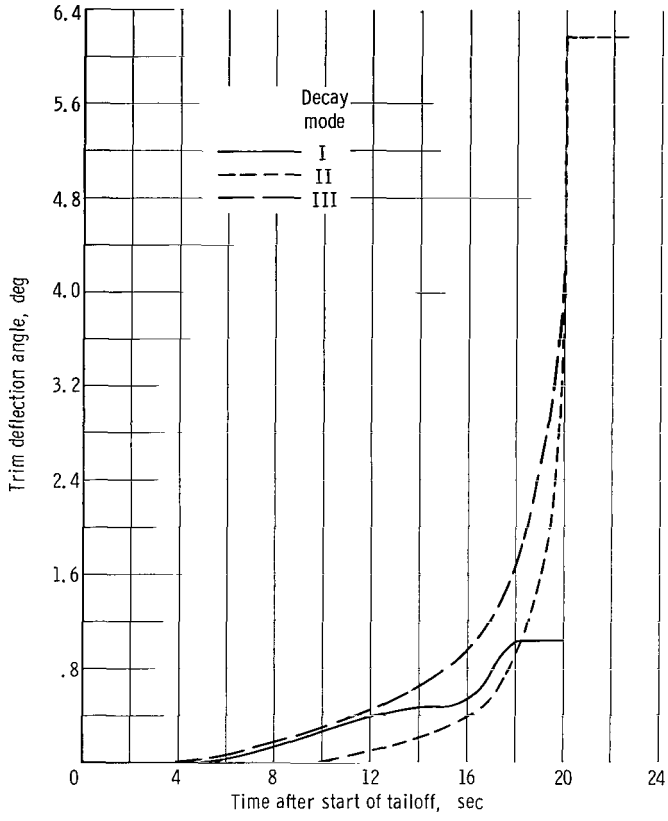

Figure 22. - Thrust-vector deflection requirements during tailoff for SSOPM.

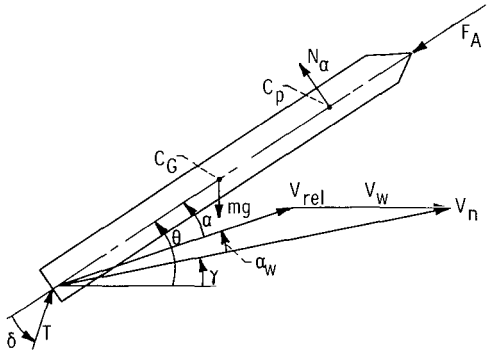

Figure 23. - Definition of trajectory and control variables for pitch plane.

NASA-Langley, 1968 —— 31 E-4367

"The aeronautical and space activities of the United States shall be conducted so as to contribute . . . to the expansion of human knowledge of phenomena in the atmosphere and space. The Administration shall provide for the widest practicable and appropriate dissemination of information concerning its activities and the results thereof."

—NATIONAL AERONAUTICS AND SPACE ACT OF 1958

NASA SCIENTIFIC AND TECHNICAL PUBLICATIONS

TECHNICAL REPORTS: Scientific and technical information considered important, complete, and a lasting contribution to existing knowledge.

TECHNICAL NOTES: Information less broad in scope but nevertheless of importance as a contribution to existing knowledge.

TECHNICAL MEMORANDUMS: Information receiving limited distribution because of preliminary data, security classification, or other reasons.

CONTRACTOR REPORTS: Scientific and technical information generated under a NASA contract or grant and considered an important contribution to existing knowledge.

TECHNICAL TRANSLATIONS: Information published in a foreign language considered to merit NASA distribution in English.

SPECIAL PUBLICATIONS: Information derived from or of value to NASA activities. Publications include conference proceedings, monographs, data compilations, handbooks, sourcebooks, and special bibliographies.

TECHNOLOGY UTILIZATION PUBLICATIONS: Information on technology used by NASA that may be of particular interest in commercial and other non-aerospace applications. Publications include Tech Briefs, Technology Utilization Reports and Notes, and Technology Surveys.

Details on the availability of these publications may be obtained from:

SCIENTIFIC AND TECHNICAL INFORMATION DIVISION

NATIONAL AERONAUTICS AND SPACE ADMINISTRATION

Washington, D.C. 20546